

# Growth and yield models for *Eucalyptus nitens* plantations in Tasmania and New Zealand

S.G. Candy  
Forestry Tasmania  
e-mail: Steve.Candy@forestry.tas.gov.au

## Abstract

A suite of empirical growth and yield models has been constructed using data from permanent plots from a number of sources in Tasmania and New Zealand. Plots include those which form part of experiments to evaluate thinning/pruning regimes or altitude effects on growth as well as sample growth plots. Stand models of mean dominant height (MDH), basal area, volume and mortality are given. An individual-tree model of basal area increment which is compatible with the stand basal area model, and a model of the relationship between total height and diameter (at breast height) are also given. Site index can be predicted from the MDH model and is defined as MDH at age 15. The stand basal area model is a modification of Clutter's projection model which includes effects due to age at thinning and thinning intensity. A model which predicts stand basal area at age 10 for unthinned stands with stocking between 900 and 1100 stems/ha is also given to facilitate simulation of the growth of hypothetical stands given only site index. Stands can be 'grown' forwards or backwards from age 10 and various thinning regimes applied if required. When this suite of models is combined with a stem taper model, yield by product type can be predicted by 'growing-on' inventory or experimental plots. Model fitting used mixed-model methodology and included a nonlinear mixed-model fitting procedure developed for this study to fit the stand basal area projection model.

## Introduction

Shining gum (*Eucalyptus nitens*) and Tasmanian blue gum (*E. globulus*) are the

major plantation species grown for pulpwood production in Australia (Whyte 1992). *Eucalyptus nitens* is preferred over *E. globulus* at higher elevations due to its greater frost tolerance (Hallam *et al.* 1989; Turnbull *et al.* 1993). Current plantings of *E. nitens* in Tasmania total approximately 54 000 ha while in New Zealand the main *Eucalyptus* species planted is *E. nitens*, with about 4000 ha planted in the central North Island and Southland mainly for short fibre pulp and chip production (Macalister 1995). Interest in sawlog regimes for *E. nitens* has also increased in south-eastern Australia with the need to find additional sources of hardwood timber (Gerrand *et al.* 1997).

This project was initiated to facilitate yield regulation for the increasing area of *E. nitens* plantations in south-eastern Australia and New Zealand. The models described here are best suited to projecting yields from inventory or experimental plots (Candy and Gerrand 1997) in existing stands from approximately age three onwards. Simulations of hypothetical stands for silvicultural regime evaluation can be carried out using the models if an estimate of site index is available.

When this suite of models is combined with a stem taper model, yield by product type can be predicted by 'growing-on' inventory or experimental plots. Candy and Gerrand (1997) use the models described here to grow on a series of thinning and pruning trial plots of *E. nitens* in Tasmania, carry out log assortments, and simulate financial returns to the grower.

## Data

Data were supplied by:

- Forestry Tasmania;
- North Forests Burnie;
- Forests and Forest Industry Council (FFIC) (Gerrand *et al.* 1997);
- CSIRO Division of Forestry (Beadle and Turnbull 1986; Turnbull *et al.* 1988; Beadle *et al.* 1989); and
- Management of Eucalypts Cooperative (MEC, administered by the Forest Research Institute, New Zealand).

### *Mensurational differences between Australia and New Zealand*

Some of the standard mensurational quantities are defined differently in New Zealand and Australia. The key differences for this study were in the definition of diameter at breast height (DBH) and dominant height. Diameter at breast height is over-bark for the remainder of this study while tree, and therefore stand, volume are under-bark values. Dominant height is defined in New Zealand as either mean top height (MTH) or predominant mean height (PDH) (Goulding 1986) where PDH is the mean height of the tallest tree on each 0.01 ha section of the plot (i.e. mean of the tallest 100 trees per hectare) and MTH is the height predicted by the Petterson function (Goulding 1986) for a DBH corresponding to the quadratic mean DBH of the 100 largest trees (based on DBH) per hectare. Mean dominant height (MDH) is the Australian standard defined similarly to PDH except that the rate at which MDH trees are selected is 50 per hectare, or one per 0.02 ha plot section, instead of 100.

In this study, a simple empirical conversion has been developed by calculating MTH, PDH, and MDH where possible (i.e. if a sample of tree heights is available for the measurement) for each New Zealand plot. Regression relationships were then developed as given below:

$$\begin{aligned} \text{MDH} &= 0.0065 + 1.10367\text{PDH} \\ \text{MDH} &= -0.0906 + 1.0311\text{MTH}. \end{aligned}$$

The  $R^2$  for the PDH to MDH regression was 0.999, with error mean square of 0.0984, while for MTH to MDH, the  $R^2$  was 0.996, with error mean square of 0.2841. The suite of models described here use MDH, so conversion to this standard is required before the models can be applied.

The other difference is in the definition of 'breast height' for measurement of diameter. The New Zealand standard is 1.4 m above ground while the Australian standard is 1.3 m. The definition applied in this study for breast height was 1.3 m for DBH and basal area. The New Zealand measured DBHs were converted to the 1.3 m standard (i.e. a slight increase of the New Zealand DBH) (method by A. Gordon, pers. comm.) using an *E. nitens* taper model. A simple conversion to give  $\text{DBH}_{1.3}$  from  $\text{DBH}_{1.4}$ , which is sufficiently accurate for most practical applications, was obtained by regression using all New Zealand measured  $\text{DBH}_{1.4}$ s in the data and corresponding estimated  $\text{DBH}_{1.3}$ s. The regression equation is

$$\text{DBH}_{1.3} = 0.13 + 1.0036\text{DBH}_{1.4}$$

with an  $R^2$  of 0.999 and standard error of prediction of 0.064 cm (ignoring regression parameter estimation error).

Individual-tree entire stem volume was calculated using a New Zealand *E. nitens* taper model, aggregated for all trees on the plot, and then scaled by plot area to give stand volume,  $V$ .

### *Data summaries*

Summaries of the data are given in Tables 1 and 2. Figure 1 shows the age distribution of plot measurements over all plots (a) and by plot (b).

### **Statistical methods**

Extensive use has been made of mixed-model methods in developing the models reported here. Mixed models allow nested and crossed random effects to be included in regression

Table 1. Number of plots and plot/measurements by data source.

Data source	Area of plots (or range) (ha)	Number of plots	Number of measurements			Total measurements
			mean	min	max	
North Forests	0.04	68	6.2	2	13	419
MEC (New Zealand)	0.01-0.30	96	3.3	2	9	321
FFIC	0.10	51	4.1	3	5	210
Forestry Tasmania	0.056-0.062	5	4.6	4	5	23
CSIRO	0.02	8	5.0	5	5	40

Table 2. Summary of stand and thinning data. (V = volume, MAI = mean annual increment, MDH = mean dominant height) (Table 2b: FFIC = Forests and Forest Industry Council)

(a) Stand data.

	Age (yrs)	V (m <sup>3</sup> /ha)	MAI (m <sup>3</sup> /ha/yr)	Altitude (m)	Initial stocking (stems/ha)	Site index (age 15)	MDH (m)	Measurement interval (yrs)
Mean	7.4	90.4	10.7	337	1142	26.2	14.7	1.3
Minimum	2.0	0.7	0.4	60	100	13.8	1.8	0.2
Maximum	34.0	742.9	42.4	860	2600	38.9	35.5	11.5

(b) Thinning data. (Fifty plots thinned once. Figures in brackets are for the 32 FFIC thinned plots.)

	Age at thinning	Stems retained (stems/ha)	% Basal area removed
Mean	6.3 (4.7)	289 (247)	58.4 (60.3)
Minimum	3.1 (3.1)	80 (80)	23.3 (23.3)
Maximum	29.0 (7.0)	825 (410)	88.6 (88.6)

models taking into account to some degree the correlation between successive measurements on sample units (West *et al.* 1984) which, in this case, are permanent growth or experimental plots. Developed originally for linear models, mixed models have since been expanded to incorporate generalised linear models (GLM) (McCullagh and Nelder 1989) and are abbreviated GLMMs (Schall 1991; Engel and Keen 1994; Wolfinger and O'Connell 1993; Breslow and Clayton 1993) and nonlinear models (NLMMs) (Lindstrom and Bates 1990; Vonesh and Carter 1992; Davidian and Gallant 1993; Wolfinger 1993). Gregoire *et al.* (1995) used a linear mixed model (LMM) which included random plot effects and a continuous-time autoregressive conditional error structure

to model stand basal area of Douglas fir and white pine. Here, the projection form of a stand basal area model (Clutter *et al.* 1983) is used and random plot effects incorporated into the nonlinear structure of the model. An 'iterated REML' procedure is used for this NLMM similar to that described by Candy (1997) for composite link GLMMs which are intermediate between GLMMs and NLMMs in degree of nonlinearity (see also McGilchrist 1994). The method developed here to fit the stand basal area projection model as a NLMM is similar to that of Lindstrom and Bates (1990) in that it iterates between a Taylor series expansion of the nonlinear model and a fit of the resulting approximate LMM but it differs in an important way from their method. That is,

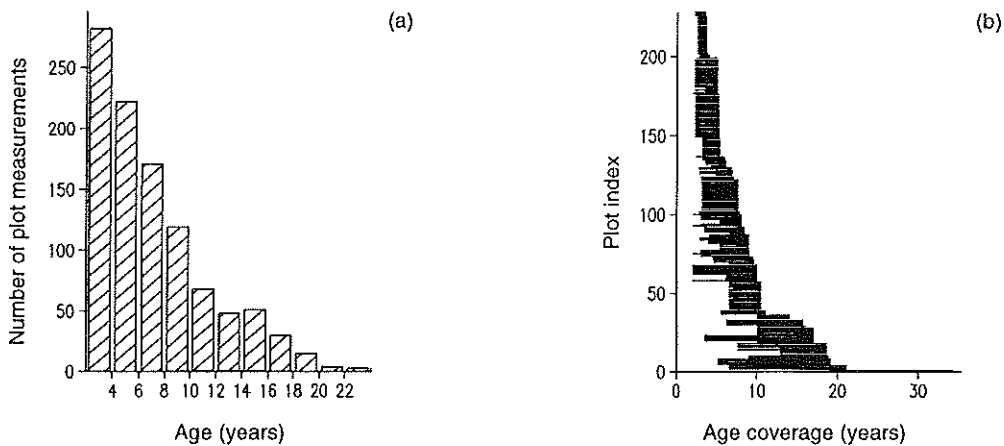


Figure 1. Distribution of age at measurement. (a) Histogram and (b) age coverage for individual plots.

the marginal rather than subject-specific form of the model is fitted here (see below and Appendix 1). The models of mortality, stand volume, and parameters of the individual-tree models were each fitted as GLMMs using the Genstat (Genstat 5 Committee 1993) GLMM procedure (Payne *et al.* 1993).

The use of mixed models is particularly important when hypothesis testing is required (under the mixed model) since ordinary least squares (OLS) estimates of parameter standard errors and the residual mean square are known to be biased downwards for repeated measurements data. The stand basal area, mortality, and individual-tree models of basal area increment and total height each required extensive hypothesis testing to determine if inclusion of extra covariates such as site index, altitude, and thinning terms (in the stand basal area model) were necessary. For the MDH increment and stand-volume models, hypothesis testing was unnecessary since the form of these models is well established. The marginal rather than subject-specific (SS) form (Zeger *et al.* 1988; Breslow and Clayton 1993; Candy 1997) of the GLMM and NLMM were used to provide population-average parameter estimates (Zeger *et al.* 1988; Schabenberger and Gregoire 1996) since parameter estimates for the SS model are biased when used to predict the average value of the response given the covariates.

### MDH increment/site index model

The state-space (Garcia 1994) or projection form of the Richards model was used to model MDH (=  $H$ ) (Model 1). The equation for obtaining site index given an MDH of  $H$  at age  $T$  is obtained by substituting  $H$  for  $H_1$ ,  $T$  for  $T_1$ , and 15 for  $T_2$  in Model 1, with  $H_2$  then corresponding to site index (base age 15).

Model 1 was fitted using nonlinear least squares using Genstat's FITNONLINEAR directive. The data were first arranged into measurement pairs  $\{H_2, H_1\}$  at ages  $\{T_2, T_1\}$ , with  $H_2$  the response variable which represents MDHs at measurement 2 to the last measurement on each plot.  $H_1$  represents the MDH at the start of each projection period at age  $T_1$ . For a more rigorous notation we could replace the index 2 by  $k+1$  and the index 1 by  $k$ , where  $k = 1, \dots, m-1$  and  $m$  is the number of measurements on the plot (Candy 1989), but the simpler notation given by the measurement pairs above will be used throughout. This approach to fitting corresponds to the state-space (Garcia 1994) or projection form of the model (Clutter *et al.* 1983).

Unfortunately, the fitting algorithm did not converge, with the difficulty identified as the inability to estimate the asymptote,  $A$ . The young ages of most of the plot measurements meant that the MDH trajectories with age

### Model 1

$$H_2 = A \left[ 1 - \left\{ 1 - \left( \frac{H_1}{A} \right)^{1/\alpha} \right\}^{\frac{T_2}{T_1}} \right]^\alpha \quad (1)$$

where  $T_1$  is the age at the start and  $T_2$  the age at the end of the projection period,  $H_1$  is the MDH at the start and  $H_2$  the MDH at the end of the projection period,  $A$  is the parameter representing the asymptotic MDH and  $\alpha$  is a shape parameter.

### Model 2

$$\ln(B_2) = \left( \frac{T_1}{T_2} \right)^{\alpha_2} \ln(B_1) + \left( \frac{\alpha_0}{\alpha_2} + \frac{\alpha_1}{\alpha_2} S \right) \left[ 1 - \left( \frac{T_1}{T_2} \right)^{\alpha_2} \right] \quad (2)$$

where  $(B_2, B_1)$  are the stand basal areas giving response and conditioning variable defined in the same way as those given for MDH. Stand basal area  $B_2$  is net basal area; that is, it excludes trees that have died in the projection period.

were approximately linear. When  $A$  was fixed at one value in a range of 50 and 75 m, the shape parameter could be successfully estimated and the minimum residual sum of squares (RSS) was obtained for  $A = 50$ . This is an unrealistically low asymptote, considering that some plots already had MDHs of as much as 35 m by age 15. To overcome this difficulty, the asymptote for the remainder was set at 60 m and the shape parameter estimate of 0.9113 was obtained with standard error 0.0174. This model accounted for 97.1% of the variance in MDH, with residual mean square (RMS) of 1.325. Figure 2a shows the residuals  $H_2 - \hat{H}_2$  (where  $\hat{H}_2$  is the value estimated from (1)) versus age,  $T_2$ . Figure 2b shows the same residuals versus the fitted values,  $\hat{H}_2$ . Figure 3a shows the set of site index curves derived from (1) while Figure 3b includes the observed MDH trajectories.

Site index is required as a predictor variable in some of the models described below. An estimate of site index can be obtained at each measurement of each plot in the dataset.

However, site index would then vary with age, which contradicts the intent that site index be a measure of site productivity. So, for the remainder, site index,  $S$ , was estimated using the measurement age closest to the index age of 15, and this estimate was used for all measurement periods for the particular plot to calibrate the models which rely on site index as input.

### Stand basal area projection model

The basic form of the model used (i.e. excluding thinning effects) is given by equations (4.42) and (4.43) in Clutter *et al.* (1983). The stand basal area,  $B$ , instantaneous growth rate function is

$$\frac{dB}{dT} = T^{-1}B[\alpha_0 + \alpha_1 S - \alpha_2 \ln(B)]$$

where  $\alpha_0$ ,  $\alpha_1$ ,  $\alpha_2$  are parameters to be estimated and  $S$  is site index as defined earlier. The projection form of the model, which is at this stage a state-space model, is given by Model 2.

Model 2 is consistent (i.e.  $B_2 = B_1$  if  $T_2 = T_1$ ) and path invariant. The property of path invariance ensures that the same predicted value of  $B$  is obtained irrespective of the number of intermediate ages at which  $B$  is predicted (Clutter *et al.* 1983) and is a function of the state-space definition of (2). However, this property needs qualification when a thinning has been carried out or is simulated. If a thinning occurs at age  $T_t$ , then for projections of  $B_2$  after thinning,  $B_1$  in (2) should be set to the residual basal area at the thinning age (or initialised at a later age if inventory is at age  $T_1 \geq T_t$ ).

Model 2 has two less desirable features. Firstly, the growth rate (1) is not defined at age zero and, as a result, a starting basal area is required in (2) to obtain a yield curve for a given site index. The yield curve corresponding to (2) is given by

$$B = \exp\left(\frac{\alpha_0}{\alpha_2} + \frac{\alpha_1}{\alpha_2} S + \beta T^{-\alpha_2}\right)$$

with the projection model (2) derived from the yield equation by solving for  $\beta$  in terms of initial age,  $T_1$ , and basal area,  $B_1$ . So starting values of basal area and age as well as site index are required to determine the

yield curve. Secondly, if  $\ln(B_1) > \frac{\alpha_0}{\alpha_2} + \frac{\alpha_1}{\alpha_2} S$ ,

then the relative growth,  $\ln(B_2) - \ln(B_1)$ , is

negative. Since the right hand side of the above inequality is the logarithm of the asymptotic basal area, then theoretically this inequality should never be satisfied. However, the asymptote must be estimated and it is possible that a measured basal area is greater than the estimated asymptote but this is unlikely to occur in practice. Candy (1989, 1997) obtained a projection model from the same instantaneous growth rate function by solving for the asymptote rather than  $\beta$  and then modelling the  $\beta$  and  $\alpha_2$  parameters as functions of site index and other stand variables. The above inequality can never occur with this 'anamorphic' projection model. However, Clutter's 'polymorphic' projection model (2) gave a superior fit to the dataset here so it was preferred over the anamorphic projection model.

The above properties of Model 2 do not, in general, limit its utility as discussed later.

#### Thinning effects

The simplest way to handle the effect of thinning is to assume that there is no effect of thinning on relative growth (i.e. 'grow on' the residual basal area after thinning using (2)). Alternatively, thinning may affect relative growth compared to an unthinned stand of the same initial basal area, initial age, and site index. Commonly, thinning effects are incorporated in basal area projection models

### Model 3

Let 'linear age components' be

$$\eta_1 = T_1 + \alpha_3 P_t + \alpha_4 P_t T_t + \alpha_5 P_t T_t S$$

$$\eta_2 = T_2 + \alpha_3 P_t + \alpha_4 P_t T_t + \alpha_5 P_t T_t S$$

$$\text{then } \ln(B_2) = \left(\frac{\eta_1}{\eta_2}\right)^{\alpha_2} \ln(B_1) + \left(\frac{\alpha_0}{\alpha_2} + \frac{\alpha_1}{\alpha_2} S\right) \left\{1 - \left(\frac{\eta_1}{\eta_2}\right)^{\alpha_2}\right\} \quad (3)$$

where  $P_t$  is the proportion of basal area removed in thinning at age  $T_t$ .

using combinations of age, intensity and nature of thinning (Bailey and Ware 1983; Pienaar and Shiver 1986; Candy 1989). Bailey and Ware (1983) incorporate thinning effects in Model 2 with the constraint that  $\alpha_2 = 1$ . The yield model in this case is a simple log/reciprocal model which is often not flexible enough to model yield or increment, which is the reason Clutter *et al.* (1983) introduced the

extra parameter,  $\alpha_2$ . Bailey and Ware (1983) define a thinning variable,  $R_t$ , as the ratio of the quadratic mean DBH of stems removed,  $D_t$ , to the quadratic mean DBH of all stems prior to thinning,  $D_b$ , (i.e.  $R_t = \frac{D_t}{D_b}$ ). Here, thinning was incorporated in (2), while maintaining path invariance according to Model 3.

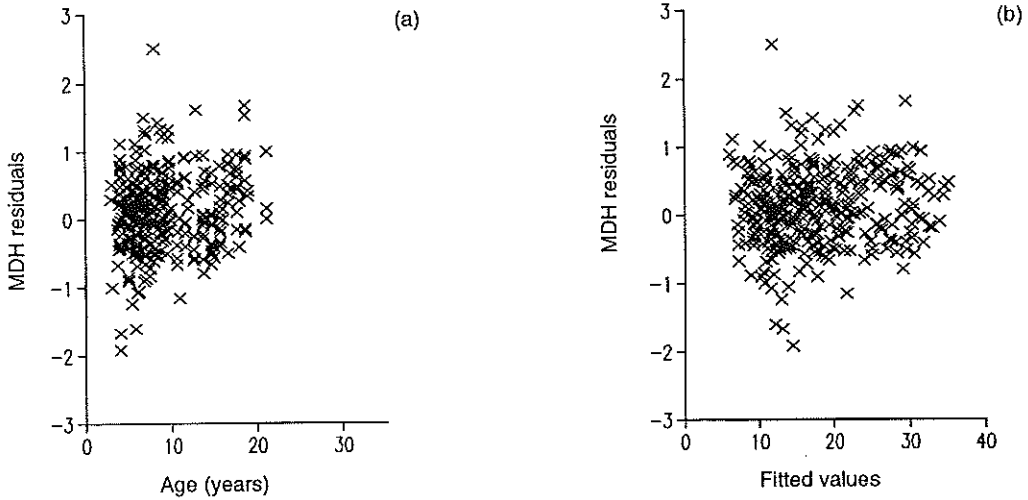


Figure 2. Residuals for MDH versus (a) age and (b) fitted values.

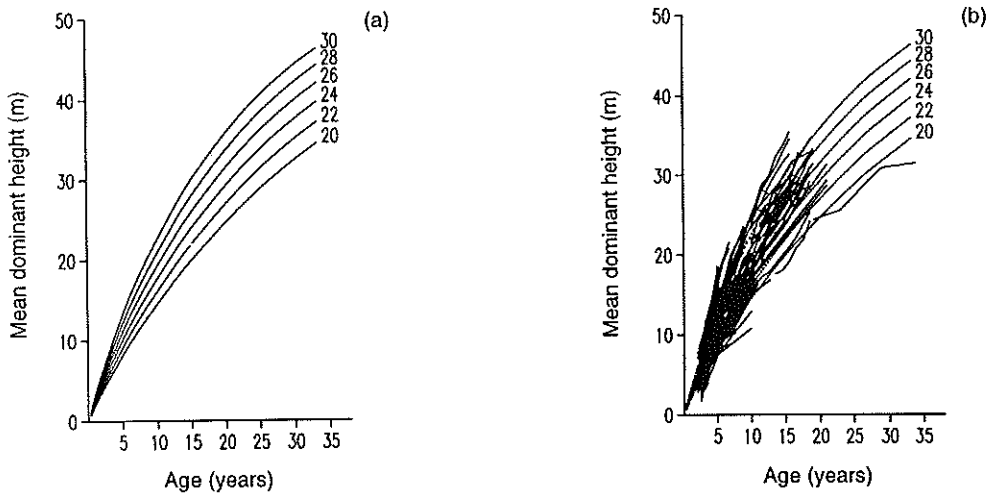


Figure 3. Site index curves (a) excluding observed MDH growth trajectories, and (b) including observed MDH growth trajectories.

For unthinned stands or ages prior to thinning in thinned stands,  $P_t$  and  $T_t$  are each set to zero. After thinning,  $P_t$  and  $T_t$  remain fixed at their thinning-age values for all later projection periods unless another thinning is applied, in which case they are changed to this later thinning's values (note that the data used here involved, at most, one thinning). As described earlier, the age at thinning should start a new projection period with  $T_1 = T_t$  and  $B_1$  set to the retained basal area. It can be seen that these thinning terms affect growth by modifying the age terms in (2). Depending on the age and intensity of thinning and the sign and magnitude of the parameters  $\alpha_3$ ,  $\alpha_4$  and  $\alpha_5$ , the 'age shift' may be to an earlier or later age. Since growth rate depends on age, as in (2), then relative growth may be increased or decreased by thinning. Since Model 3 is purely an empirical construct, expression of the effect of thinning in relative basal area growth depends largely on the available thinning data. Note that Model 3 no longer has a state-space representation since, given  $T_1 > T_t$ , future values of the state variable, stand basal area, do not depend solely on the state variables (i.e. at age  $T_1$ ).

#### Model fitting

The response variable in the fit of Model 3 was  $\ln(B_2)$ . Since the calibration data involved repeat measurements of sample growth/experimental plots, a mixed model was constructed from (3) by adding random plot effects to the linear age and site index components of the model. At the same time, to facilitate the fitting procedure, the parameters in the linear site index term,

$$\frac{\alpha_0}{\alpha_2} + \frac{\alpha_1}{\alpha_2} S, \text{ were reparameterised as } \alpha_0 + \alpha_1 S.$$

The nonlinear mixed model (NLMM) is then given by Model 4.

The random effects have zero expected values, and variances and covariances as follows:

$$\text{Var}(b_{1i}) = \sigma_1^2, \text{Var}(b_{2i}) = \sigma_2^2, \text{Cov}(b_{1i}, b_{2i}) = 0.$$

It was found that iterative weights given by

$$w_i = \left\{ 1 - \left( \frac{\eta_{1i}}{\eta_{2i}} \right)^{\alpha_2} \right\}^{-2}$$

were required in the fit, since residuals given

by  $\left\{ \ln(B_{2i}) - \hat{\ln}(B_{2i}) \right\} w_i^{\frac{1}{2}}$  showed no evidence

of increasing variance when plotted against

$w_i^{\frac{1}{2}}, \ln(B_{2i}) - \ln(B_{1i})$ , or  $T_2 - T_1$ , which was not the case with raw residuals,

$\ln(B_{2i}) - \hat{\ln}(B_{2i})$ . The variance of  $\varepsilon_{2i}$  was therefore assumed to be  $\sigma^2 w_i^{-1}$ .

The fitting procedure involved linearising (4) using a first-order Taylor series expansion and iteratively fitting the linear mixed model of the form given by Model 5.

In (5), working vectors and matrices, with the exception of  $\mathbf{e}$ , are functions of the current iteration's estimate of the fixed effects,  $\alpha$ , and observed covariates, and are therefore updated at each iteration (see Appendix 1). If the random effects estimates are included in the calculation of  $\mathbf{X}$  and  $\mathbf{Z}$ , the fitted model is called a 'subject-specific' (SS) model. If the SS fixed-effect estimates are used to predict the average value of the response ( $\ln(B_{2i})$  here) given the covariates in a GLMM or NLMM, the predictions will be biased (Zeger *et al.* 1988; Lindstrom and Bates 1990). To overcome this problem, Breslow and Clayton (1993) proposed the 'marginal model' for GLMMs. The corresponding marginal model in this case is obtained by excluding the random-effects estimates from the calculation of  $\mathbf{X}$  and  $\mathbf{Z}$  while using (5) to obtain the marginal variance-covariance matrix for  $\mathbf{y}$ . This 'marginal model' is the model described below. The fitting algorithm is given in detail in Appendix 1.

Table 3 gives the parameter estimates and their standard errors for Model 3, fitted using (4) and (5), along with some statistics from



Table 3. Parameter estimates for the stand basal area projection model.

Parameter	$\alpha_0$	$\alpha_1$	$\alpha_2$	$\alpha_3$	$\alpha_4$	$\alpha_5$
Estimate	3.53173	0.03442	0.85751	6.78663	1.69372	-0.09569
Standard error	0.27420	0.00880	0.07036	1.18531	0.83092	0.02952
Fit statistics	Value/estimate		Standard error		Effective df	
RSS{ $\ln(B_{2i})$ }	5.330		-		592.00	
$\hat{\sigma}_1^2$	0.1222		0.0283		158.55	
$\hat{\sigma}_2^2$	3.3931		1.0230		78.23	
$\hat{\sigma}^2$	0.2714		0.0204		355.27	

#### Model 4

$$\eta_{1i} = T_{1i} + \alpha_3 P_{1i} + \alpha_4 P_{1i} T_{1i} + \alpha_5 P_{1i} T_{1i} S_i + b_{2i}$$

$$\eta_{2i} = T_{2i} + \alpha_3 P_{2i} + \alpha_4 P_{2i} T_{2i} + \alpha_5 P_{2i} T_{2i} S_i + b_{2i}$$

$$\ln(B_{2i}) = \left( \frac{\eta_{1i}}{\eta_{2i}} \right)^{\alpha_2} \ln(B_{1i}) + (\alpha_0 + \alpha_1 S_i + b_{1i}) \left\{ 1 - \left( \frac{\eta_{1i}}{\eta_{2i}} \right)^{\alpha_2} \right\} + \varepsilon_{2i} \quad (4)$$

where the  $i = 1, \dots, n$  subscript is introduced to represent the  $i$ th plot in a total of  $n$  plots and  $b_{1i}$  and  $b_{2i}$  are random plot effects with  $n$  elements each and  $\varepsilon_{2i}$  is a random error independent of the random effects.

#### Model 5

$$\mathbf{y} = \mathbf{X}\boldsymbol{\alpha} + \mathbf{Z}\mathbf{b} + \mathbf{e} \quad (5)$$

where  $\mathbf{b}$  is a stacked vector which contains the random effects and  $\mathbf{y}$ ,  $\mathbf{X}$ ,  $\mathbf{Z}$  and  $\mathbf{e}$  are working response vector, working fixed effect design matrix, working random effect design matrix, and within-plot random error vector respectively (Candy 1997).

the fit. The dataset used in the fit consisted of 598 measurement pairs which excluded pairs for which  $T_{1i}$  was less than three years. These younger measurements were excluded since it was considered that they would be too highly dependent on vagaries of plantation

establishment and would not necessarily reflect the site's growth potential. Also, the measurements after thinning of a single plot which was thinned from 388 stems/ha to 200 stems/ha at age 29 were excluded from the fit since these data points have very high

leverage on the parameter estimates in the thinning terms if included, and thinning at such a late age is not a serious proposition. Figure 4 shows marginal (i.e. excluding random effects) raw residuals,

$$\left\{ \ln(B_{2i}) - \hat{\ln}(B_{2i}) \right\}, \text{ versus each of } w_i^{-1/2} \text{ and}$$

$\hat{\ln}(B_{2i})$ . Figure 5a shows standardised marginal residuals

$$\left\{ \ln(B_{2i}) - \hat{\ln}(B_{2i}) \right\} \left[ \hat{\text{Var}}\{\ln(B_{2i})\} \right]^{-1/2} \text{ versus } w_i^{-1/2}$$

and Figure 5b shows the same residuals

versus  $\hat{\ln}(B_{2i})$ , where

$$\hat{\text{Var}}\{\ln(B_{2i})\} = \hat{\sigma}_1^2 z_1^2 + \hat{\sigma}_2^2 z_2^2 + w^{-1} \hat{\sigma}^2,$$

$$z_1 = \hat{w}^{-1/2}, \text{ and}$$

$$z_2 = \hat{\alpha}_2 \left( \frac{\hat{\eta}_1}{\hat{\eta}_2} \right)^{\hat{\alpha}_2 - 1} \frac{\hat{\eta}_2 - \hat{\eta}_1}{\hat{\eta}_2^2} \{ \ln(B_1) - (\hat{\alpha}_0 + \hat{\alpha}_1 S) \}.$$

Figure 5c shows conditional (i.e. including random effects obtained from the fit of the SS model) raw residuals,

$$\left\{ \ln(B_{2i}) - \hat{\ln}(B_{2i} | \hat{b}_1, \hat{b}_2) \right\}, \text{ and Figure 5d shows}$$

conditional standardised residuals,

$$\left\{ \ln(B_{2i}) - \hat{\ln}(B_{2i} | \hat{b}_1, \hat{b}_2) \right\} \hat{w}_i^{-1/2} \text{ versus } \hat{w}_i^{-1/2}.$$

Figures 4, 5a and 5b show that the weighted residuals appear to have homogeneous variances while the raw residuals do not. The conditional residuals in Figures 5c and 5d indicate that although weighting has improved the homogeneity of variances it has possibly overcorrected for the trend for small variances (or spread of points) with small  $w_i^{-1/2}$ . However, it should be noted that there are far more data points for small  $w_i^{-1/2}$  so at these values the greater spread of residuals could partly reflect the greater sample size. Figure 6 shows estimated random effects,  $\hat{b}_1$  versus  $\hat{b}_2$ . It can be seen from Figure 6 that these random effects are uncorrelated. Figure 7 shows observed and predicted trajectories for stand basal area for unthinned plots which have had more than four measurements after age three. Predicted trajectories have been adjusted for back-transformation bias (see below).

The marginal variance of  $\ln(B_{2i})$  is given approximately by  $\sigma_1^2 z_1^2 + \sigma_2^2 z_2^2 + w^{-1} \sigma^2$ . The relative importance of the three variance

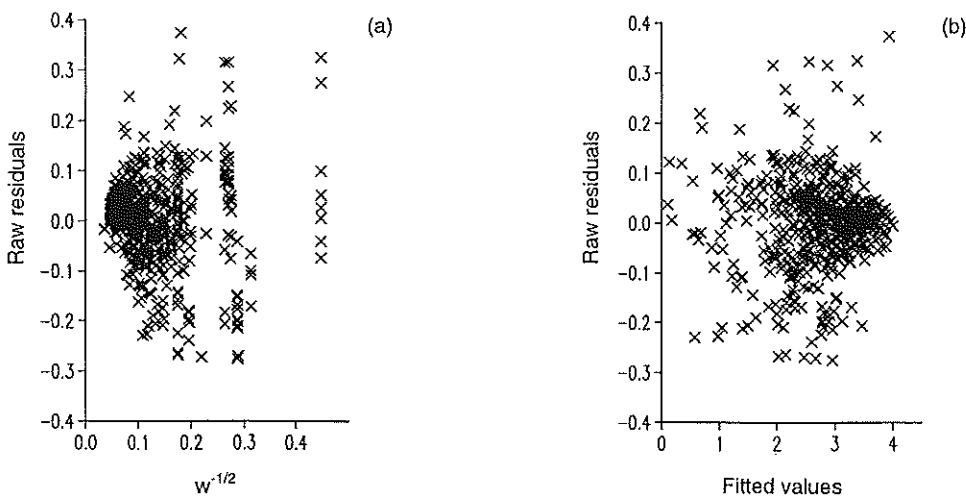


Figure 4. Basal area raw residuals versus (a)  $w^{-1/2}$  and (b) fitted values.

components was assessed by calculating their mean (over all values of  $z_1, z_2, w^{-1}$ ) percentage contribution to the total variance. These percentages were 20.2% for  $\sigma_1^2 z_1^2$ , 34.8% for  $\sigma_2^2 z_2^2$ , and 45.0% for  $w^{-1} \sigma^2$ . The mean value for the marginal variance was 0.02.

There is a well-known bias in predictions when back-transforming from the logarithmic scale, which is required for the models here which were fitted with  $\ln(B_{2i})$  as the response variable. Adjustments for back-

transformation bias for the logarithmic transformation have been proposed in the case of single error models (Flewelling and Pienaar 1981), with the simplest and most commonly used adjustment obtained by multiplying the back-transformed basal area by the term  $\exp(0.5\sigma^2)$ , where  $\sigma^2$  is the residual mean square from regression. Appendix 2 gives a derivation for the analogous adjustment for the mixed model described above, taking into account the weights  $w_i$ . The adjusted prediction of stand basal area is derived as Model 6.

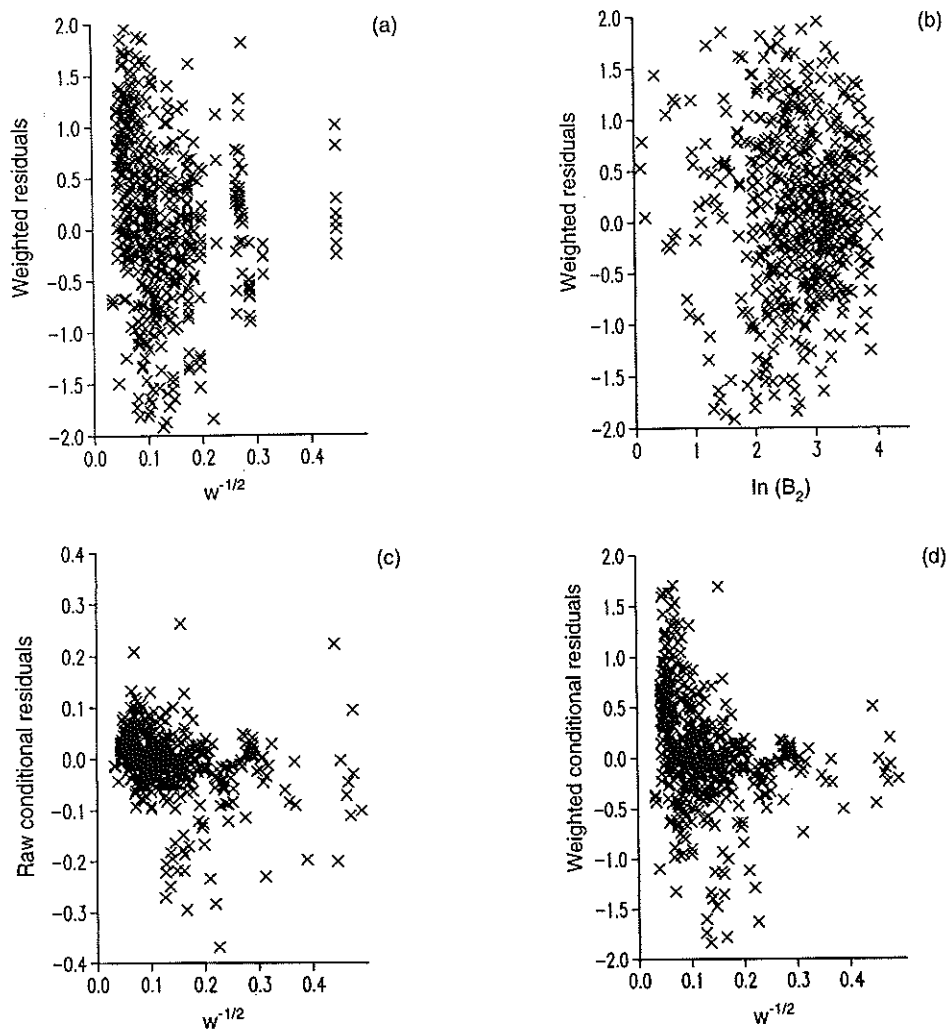


Figure 5. Basal area weighted marginal residuals versus (a)  $w^{-1/2}$  and (b)  $\ln(B_2)$ , and conditional raw (c) and weighted (d) residuals versus  $w^{-1/2}$

The terms  $\hat{\sigma}_2^2 z_2^2$  and  $\hat{w}^{-1} \hat{\sigma}^2$  in (6) are largely dependent on the ratio  $\frac{\hat{\eta}_1}{\hat{\eta}_2}$  which, for unthinned stands, is the ratio of age of prediction to start age for the projection period. For example, for an unthinned stand with  $T_1 = 10$ ,  $T_2 = 11$ ,  $S = 30$ ,  $B_1 = 35.13$ , the adjustment is negligible at 1.0013 (i.e. 0.13%) but, projecting to age 30, the adjustment is 1.0765 (i.e. 7.65%). If the unadjusted prediction is used and the distribution of  $B_2$ , given  $B_1$ ,  $T_2$ ,  $T_1$  and  $S$ , is lognormal, ignoring random effects, then this prediction is a consistent estimate of the median (Gregoire *et al.* 1995). Alternatively, the adjusted value gives the mean. The unadjusted prediction may be preferable if a conservative approach is adopted. This is, however, only one of a number of issues to consider when predicting stand basal area since the models developed here are fitted to plot data from a wide range of geographical locations, with ages at plot measurement confounded with location. Therefore, the mean of predictions for a more restricted range of plot locations than the range of the calibration data will have some degree of bias.

An approximate variance for the unadjusted prediction,  $\hat{B}_2$ , ignoring estimation error in fixed effect parameters, is given by Model 7.

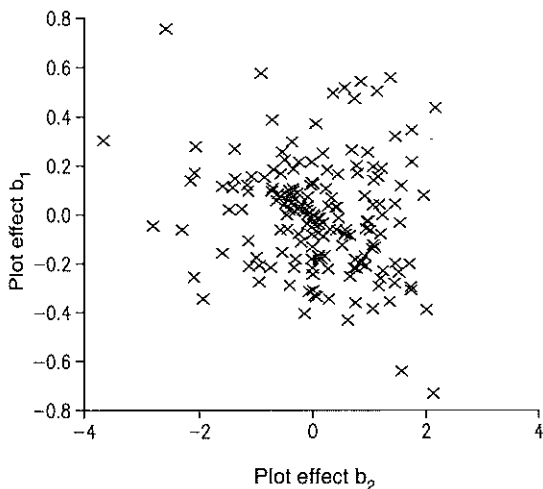


Figure 6. Estimated random plot effect  $\hat{b}_1$  versus  $\hat{b}_2$  for stand basal area NLMM.

#### Model 6

$$\tilde{B}_2 = \exp\{0.5(\hat{\sigma}_1^2 z_1^2 + \hat{\sigma}_2^2 z_2^2 + \hat{w}^{-1} \hat{\sigma}^2)\} \hat{B}_2 \quad (6)$$

where  $\hat{B}_2 = \exp\{\hat{\mu}\}$ ,  $\hat{\mu}$  represents the marginal (i.e. excluding random effect terms) fitted values from (4) given by  $\hat{\ln}(B_{2i})$ .

#### Model 7

$$\text{Var}(\hat{B}_2) \equiv (\sigma_1^2 z_1^2 + \sigma_2^2 z_2^2 + w^{-1} \sigma^2) \hat{B}_2^2 \quad (7)$$

#### Model 8

$$\ln(B_{10}) = \beta_0 + \beta_1 S^{-1} \quad (8)$$

Using the examples above to demonstrate back-transformation bias, for the age 11 prediction, the standard error derived from (7) as a percentage of the predicted basal area was 5.1%, while for the prediction at age 30 it was 38.4%. When Model 4 was fitted using ordinary least squares without weighting, the residual mean square was estimated as  $\hat{\sigma}^2 = 0.00896$ . This gives a constant percentage standard error of 9.5%. Clearly, this underestimates the standard error of predictions since the estimate of  $\sigma^2$  is biased due to the repeated measurement nature of the data, and no account is taken of the increasing error variance with increasing length of projection period. The mixed model approach with iterative weights gives more realistic error variances.

To demonstrate the effect on the fit of Model 3 of the thinning terms, the RSS for the following three models and (i) the complete dataset, (ii) measurements which were not preceded by a thinning, and (iii) measurements which were preceded by a thinning are given in Table 4. The models were: (a) Model 3 fitted to all the data, (b) Model 2 fitted to all the

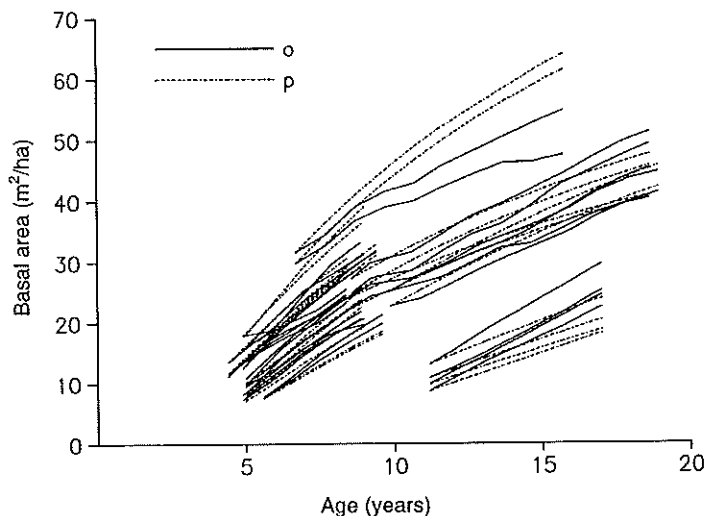


Figure 7. Observed (o) and predicted (p) basal area trajectories for unthinned plots with more than four measurements after age 3.

data, and (c) Model 2 fitted to the data defined by (ii) above. Clearly, Model 3 is superior for thinned plots and for all plots combined, while still giving as good a fit for unthinned plots as Model 2 fitted to dataset (ii). When the extended version of Bailey and Ware's (1983) model (i.e. including the  $\alpha_2$  parameter) given by

$$\ln(B_2) = \left(\frac{T_1}{T_2}\right)^{\alpha_2} \ln(B_1) + (\alpha_0 + \alpha_1 S) \left\{ 1 - \left(\frac{T_1}{T_2}\right)^{\alpha_2} \right\} + \alpha_3 X_t \left( \frac{1}{T_2^{\alpha_2}} - \frac{1}{T_1^{\alpha_2}} \right) \frac{1}{T_1 T_2^{\alpha_2}}$$

where

$$X_t = 1 - R_t; R_t > 0 \\ = 0; R_t = 0$$

was fitted to dataset (i), the fit was considerably worse than that of Model 3, with a residual sum of squares of 6.976 compared to 5.330 for Model 3 (i.e. fitted as Model 4).

Earlier it was mentioned that Model 2 has the property that relative basal area growth,  $\ln(B_2) - \ln(B_1)$ , is negative if, after reparameterisation,  $\ln(B_1) > \alpha_0 + \alpha_1 S$ . This is an undesirable property since, in the absence

of severe mortality, net stand basal area generally increases from one year to the next. However, if a low site index of 20 m is assumed and parameter estimates from Table 3 used, then  $B_1$  must be greater than  $68 \text{ m}^2/\text{ha}$  for predicted growth to be negative. In practice, for commercial regimes, it is unlikely that projecting from such high initial basal areas would be required.

#### Stand basal area at age ten

The typical use of stand projection models is to 'grow-on' inventory plots established in existing stands that are old enough for inventory to reliably represent the growth potential of the sites. Another use of these models is the growth simulation of hypothetical stands. To carry out these simulations, a starting age and corresponding MDH (or site index) and stand basal area are required. Stands can be grown forwards or backwards from this starting age. To make this task possible given only site index, a model has been constructed to predict stand basal area at age 10 ( $B_{10}$ ) for unthinned stands with stocking in the range 900 to 1100 stems/ha from a single input of site index. The data used to fit

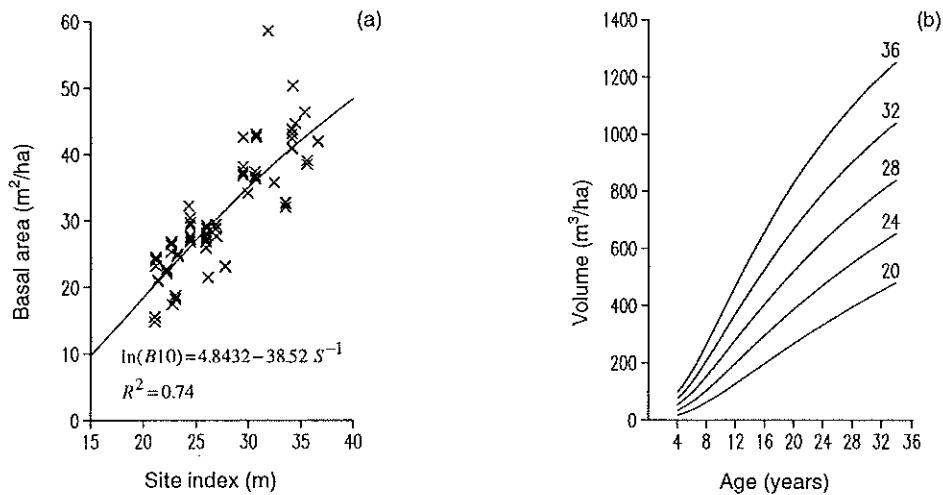


Figure 8. (a) Basal area at age 10 ( $B_{10}$ ) versus site index ( $S$ ) and (b) yield curves for site indices between 20 m and 36 m with initial basal area predicted from (a).

Table 4. Residual sum of squares for  $\ln(B_{2t})$  including or excluding thinning terms.

Data set	Number of measurements	Model (a)	Model (b)	Model (c)
Unthinned (ii)	435	4.131	5.571	4.117
Thinned (iii)	163	1.201	1.591	9.028
All data (i)	598	5.330	7.162	13.145

this model were obtained by selecting measurements for which the stocking was in the required range and no prior thinning had occurred. Then using Model 4 with parameter estimates given in Table 3, the basal area was predicted at age 10. This basal area was then regressed on site index using Model 8.

Parameter estimates, standard errors, and fit statistics including the residual mean square (RMS) are given in Table 5. Figure 8a shows the data and fitted model. Figure 8b shows yield curves for site indices of 20, 24, 28, 32 and 36 m derived by (i) obtaining initial basal area at age 10 using Model 8, (ii) projecting MDH using Model 1, (iii) projecting stand basal area using Model 4 and equation (6) for ages ranging from 4 to 36 years, and (iv) predicting stand volume from MDH and stand basal area as described below.

### Stand volume

Stand volume,  $V$ , was defined earlier as the total of individual-tree entire-stem volumes (i.e. volume from ground to tip). The Schumacher model (Model 9) was used to predict  $V$ , given measured MDH ( $H$ ) and stand basal area ( $B$ ) at any stand age.

Candy (1989) fitted the GLM version of this model (i.e. ignoring random plot effects). The marginal variance is approximately (Breslow and Clayton 1993)  $Var(V) = (\phi + \sigma_b^2) V^2$ .

Model 9 was fitted as a GLMM using the Genstat GLMM procedure (Payne *et al.* 1993) with log link function, conditional gamma error structure, and normally distributed random plot effects added to the linear predictor. The marginal method of Breslow

### Model 9

$$V = \exp\{\beta_0 + \beta_1 \ln(H) + \beta_2 \ln(B) + b\} + \varepsilon \quad (9)$$

where  $b$  is a random plot effect with variance  $\sigma_b^2$  and  $\varepsilon$  is an independent within-plot error with conditional variance  $\text{Var}(V|b) = \phi V_b^2$  where  $V_b$  is the conditional expectation of  $V$  (i.e. the right hand side of (9) excluding the within-plot error) and  $\phi$  is a dispersion parameter.

### Model 10

$$M_2 = N_1 \left\{ 1 - \exp \left[ - \int_{T_1}^{T_2} \eta(t) dt \right] \right\} + \varepsilon \quad (10)$$

where  $M_2$  is the mortality on the plot between ages  $T_1$  and  $T_2$ ,  $N_1$  is the number of live trees on the plot at age  $T_1$ , and  $\eta(t)$  is the hazard function given by

$$\eta(t) = \exp(\beta_0 + \beta_1 S + \beta_2 t + \beta_3 t^2)$$

and  $\varepsilon$  is a binomial error conditional on  $N_1$ .

Table 5. Basal area model parameter estimates and fit statistics at age 10.

Parameter	$\beta_0$	$\beta_1$
Estimate	4.8432	-38.52
Standard error	0.0950	2.47
Fit statistics		Value/estimate
RMS	0.0219	
$R^2$	0.735	

and Clayton (1993) was used in the fit. Table 6 gives the parameter estimates and some fit statistics. Figure 9a shows raw residuals and Figure 9b shows conditional Pearson residuals versus conditional fitted values,  $\hat{V}_b$ , in each case. Figure 10a shows raw marginal residuals versus marginal fitted values,  $\hat{V}_{b=0}$ . Figure 10b shows the random effects expressed as percentage adjustments to the

marginal fitted values versus plot index. Conditional raw residuals are the difference between observed and conditional fitted values (i.e. random effects estimates included) while, for marginal residuals, the conditional fitted values are replaced by marginal values (i.e. random effects estimates excluded or set to zero). Pearson (conditional) residuals (McCullagh and Nelder 1989) are simply the raw conditional residuals divided by their standard deviation excluding the dispersion parameter so that here the Pearson residual is  $(V - \hat{V}_b) \hat{V}_b^{-1}$ . It can be seen from Figure 10b that the random plot effects adjust the marginal fitted values by mostly between  $\pm 10\%$ .

### Stand mortality

The proportional hazards model (Model 10) of Candy (1989) was fitted here. Candy (1989) fitted this model as a GLM with binomial error for  $M_2$  conditional on  $N_1$ ,

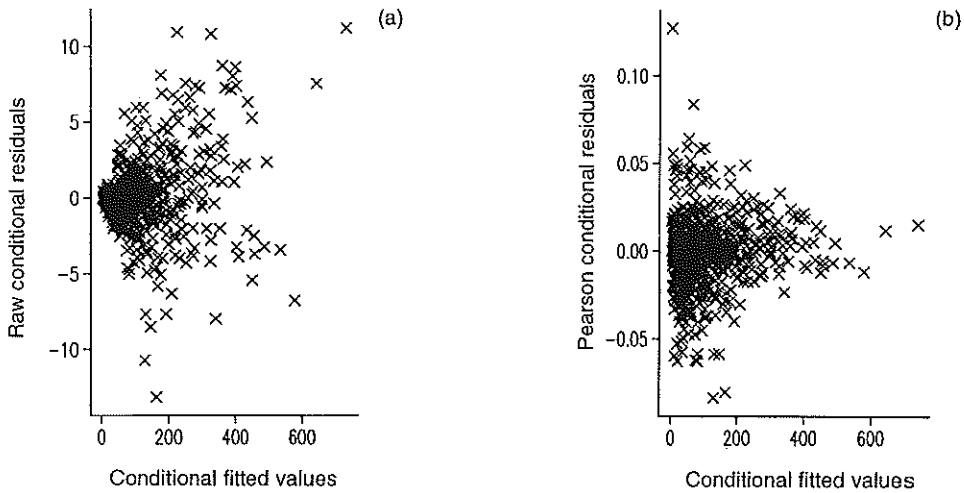


Figure 9. Stand volume conditional (a) raw and (b) Pearson residuals versus conditional fitted values.

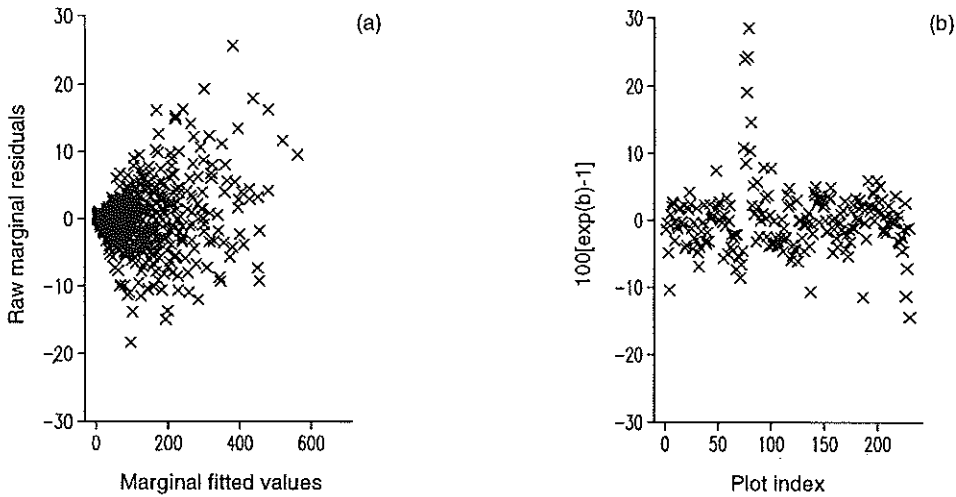


Figure 10. Stand volume (a) raw marginal residuals and (b) random plot effects expressed as a per cent deviation from the marginal fitted value.

complementary log-log link, linear predictor

$$\beta_0 + \beta_1 S + \beta_2 T_m + \beta_3 T_m^2$$

where  $T_m = (T_2 + T_1) / 2$ ,

and an offset given by  $\ln(T_2 - T_1)$ . Candy (1989) applied prior weights to scale the binomial error variance (Wedderburn 1974) but this was not done here. Instead, Model 10

was fitted as a GLMM with conditional binomial error and a random plot effect,  $b$ , within the linear predictor so the hazard function is now

$$\eta_b(t) = \exp(\beta_0 + \beta_1 S + \beta_2 t + \beta_3 t^2 + b),$$

with variance of  $b$  given by  $\sigma_b^2$ . The Genstat GLMM procedure was used to fit this model using the marginal method of Breslow and



Table 6. Stand-volume model parameter estimates and fit statistics.

Parameter	$\beta_0$	$\beta_1$	$\beta_2$
Estimate	-0.4885	0.8252	0.9682
Standard error	0.0147	0.0088	0.0047
Fit statistics	Value/estimate	Standard error	Effective df
RSS(V)	20369	-	733.00
Var( $b_1$ )	0.002560	0.000266	222.06
$\phi$	0.000573	0.000036	508.94

Table 7. Mortality volume model parameter estimates and fit statistics.

Parameter	$\beta_0$	$\beta_1$	$\beta_2$	$\beta_3$
Estimate	-8.600	0.1124	0.1487	-0.0067
Standard error	0.846	0.0232	0.1098	0.0055
Fit statistics	Value/estimate	Standard error	Effective df	
Residual deviance		-		724.00
$\sigma_b^2$	0.938	0.282		176.39
$\phi$	1.487	0.090		547.61

Clayton (1993). Table 7 gives the parameter estimates and some fit statistics. Figure 11a shows the stocking trajectories for unthinned plots used in the model fit. (Note that some slight increases in stocking are due to the ingrowth of one of a multi-leader stem to measureable size; that is, height greater than 1.3 m). Figure 11b shows predicted stocking curves for unthinned stands with 1800, 1100 and 800 initial stems/ha at age three for each of site indices 20 and 30 m.

It can be seen from Table 7 that the standard errors for the parameter estimates of  $\beta_2$  and  $\beta_3$  indicate that these terms may not be significant. However, these terms need to be retained since we know that the mortality rate is not constant with increasing age but, within a normal rotation (say less than 50 years), increases with age and then declines when the

stand 'stabilises' (Candy 1989). The parameter estimates are of a similar magnitude to those obtained by Candy (1989) for *Pinus radiata*. The main difference is the smaller magnitude for  $\beta_2$  here which means that the stocking curves tend to reach a 'stable-stand' asymptotic stocking earlier. The data available to this study are fairly limited in range of ages and stockings compared to those in Candy (1989) so refinement of this model is a high priority when sufficient later measurements of plots are available in perhaps 10 to 15 years time. Until that time, this model should be used with more caution than the other models developed here. Fortunately, density-dependent mortality is quite small for economically favourable regimes (Candy and Gerrand 1997) involving initial stockings below 1100 stems/ha, possibly combined with early non-commercial thinning or later

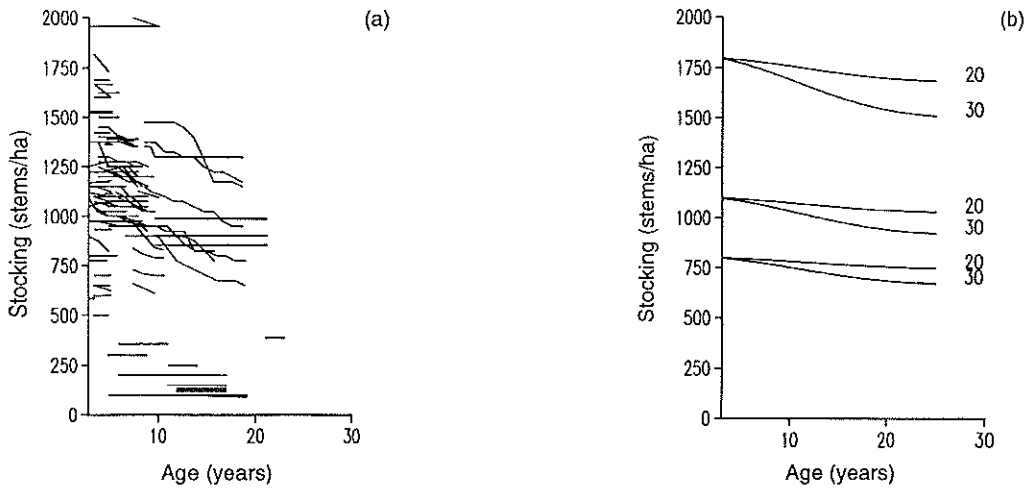


Figure 11. Stocking versus age. (a) Observed trajectories and (b) predicted trajectories for site indices of 20 and 30 and initial stockings at age 3.

(e.g. age 10 to 15) commercial thinning where stocking is reduced to a range of between 100 and 400 stems/ha.

#### Individual-tree basal area increment

To allow calculation of product assortments at commercial thinning or clearfall ages, individual-tree DBH or a distribution of DBHs is required at the projection age. One approach is to predict a DBH distribution at the projection age which, when aggregated, gives the projected stand basal area (Garcia 1984; Knoebel *et al.* 1986; Hyink and Moser 1983; Candy 1989). Yield scheduling software, in this case, does not need to retain individual-tree DBHs measured at inventory once stand basal area and volume have been calculated at the inventory age. Models which require the list of DBHs at inventory and apportion stand basal area increment directly to individual trees to give projected DBH were used by Campbell *et al.* (1979), McMullan (1979) and Woollons and Hayward (1985). There can be advantages in retaining the individual-tree attributes measured at inventory to later projection ages while projecting individual-tree DBH. As well as DBH, quality information such as pruned height, and defects such as fork height and

'top-outs' can be retained and thus give more accurate numbers and average dimensions of log products than those obtained from the DBH distribution approach. If a pre-harvest inventory is carried out and the projection period is therefore limited to say one to five years, then quality information such as branch size can be incorporated into log assortments if this information is retained. For these reasons, a DBH distribution model as, for example, in Garcia (1984) or Candy (1989) was not constructed. Instead, an individual-tree basal area increment model based on that of McMullan (1979) was constructed (Model 11). This model is a modification of McMullan's model which uses an algebraic constraint to ensure the projected DBHs reproduce the projected stand basal area (P. West pers. comm.). This constraint was incorporated into the fitting procedure with observed rather than projected  $B_2$  used in the constraint.

The constants in Model 11 are  $c$  and  $D_0$ , where  $c$  is 'constrained out' as described below and  $D_0$  is the minimum DBH below which trees are assumed to have zero increment. Model 11 without the constraint on  $c$  is simply a linear regression of  $\partial G_{2k}$  on  $D_{1k}$ , where  $c$  is the slope and  $D_0$  is the x-axis

intercept. To ensure that the projected DBHs given by  $\hat{D}_{2k}$ , where

$$\hat{D}_{2k} = 100 \sqrt{\frac{4}{\pi} (G_{1k} + \partial \hat{G}_{2k})}$$

reproduce the stand basal area, the constraint, Equation 12, is imposed on (11), where  $n_0$  is the number of trees for which  $D_{1k} > D_0$ . This means that the parameters to be estimated are those required to predict  $D_0$ . In the application of (11) and (12), since  $B_2$  is not

known, its predicted value,  $\hat{B}_2$ , obtained from Model 4 is used. The relationship between diameter increment and initial diameter from (11) is shown by Model 13, which produces a relationship between  $\partial D_{2k}$  and  $D_{1k}$  above  $D_0$  which is concave down. This gives conservative growth for the largest trees in the stand. In the author's experience, with other individual-tree models for *Pinus radiata* for which this relationship is concave up, the largest trees at inventory become unreasonably large by projected rotation ages.

#### Model 11

$$\begin{aligned} \partial \mathcal{G}_{2k} &= c(D_{1k} - D_0) ; D_{1k} > D_0 \\ &= 0 ; D_{1k} \leq D_0 \end{aligned} \quad (11)$$

where if  $G_{2k}$  is the basal area ( $m^2$ ) of the  $k$ th tree on the plot at the second measurement in the pair, and similarly  $G_{1k}$  is the basal area of the same tree at the first measurement in the pair with DBH (cm) of  $D_{1k}$ , then the individual-tree basal area increment is  $\partial \mathcal{G}_{2k} = G_{2k} - G_{1k}$ .

#### Equation 12

$$c = (B_2 - B_1) \left( \sum_{k=1}^{n_0} D_{1k} - n_0 D_0 \right)^{-1} \quad (12)$$

#### Model 13

$$\partial D_{2k} = \left[ D_{1k}^2 + \frac{4}{\pi} \partial \mathcal{G}_{2k} \right]^{\frac{1}{2}} - D_{1k} \quad (13)$$

#### Model 14

$$\hat{D}_{0(2i)}^2 = \exp(\beta_0 + \beta_1 Q_{1i} + \beta_2 Q_{1i}^2 + \beta_3 H_{1i} + \beta_4 H_{1i}^2 + \beta_5 N_{1i} + b_i) + \varepsilon \quad (14)$$

where  $Q_{1i}$  is the quadratic mean DBH given by

$$Q_{1i} = 100 \sqrt{\frac{4}{\pi} B_{1i}}$$

$b_i$  is a random plot effect with variance  $\sigma_b^2$  and  $\varepsilon$  is a gamma error.

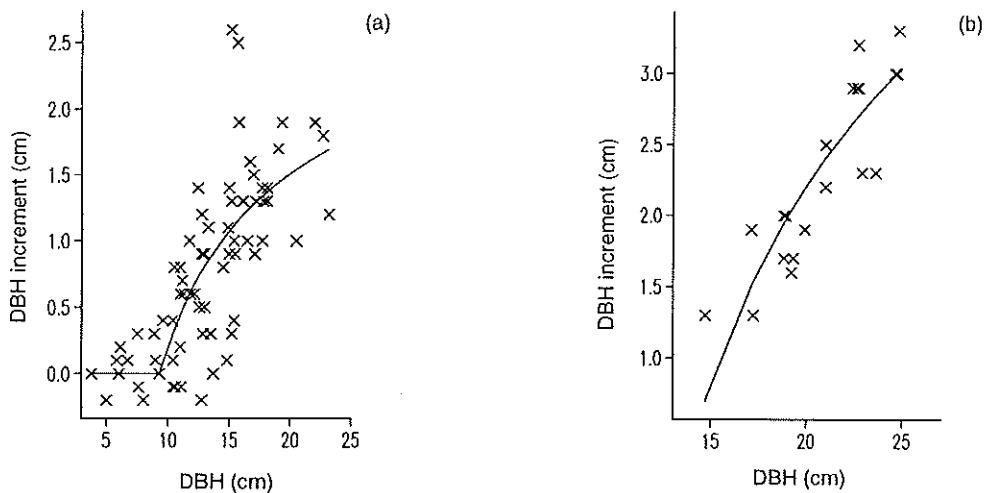


Figure 12. Observed and plot-specific predicted DBH increment for a pair of measurements from (a) an unthinned plot and (b) a thinned plot.

Table 8. Stand model for  $\hat{D}_0^2$ .

Parameter	$\beta_0$	$\beta_1$	$\beta_2$	$\beta_3$	$\beta_4$	$\beta_5$
Estimate	-1.1460	0.1530	-0.00180	0.2956	-0.00533	0.000377
Standard error	0.1737	0.0236	0.00035	0.0305	0.00061	0.000091
Fit statistics	Value/estimate		Standard error		Effective df	
Residual deviance	99.43		-		476.00	
$\sigma_b^2$	0.1808		0.0253		151.75	
$\phi$	0.0842		0.0066		324.25	

Figures 12a and 12b show the observed and predicted  $\partial D_{2k}$ , from Model 13, versus  $D_{1k}$  with  $D_0$  estimated from (11) with constraint (12) for a measurement pair for an unthinned plot (a), and a thinned plot (b).

A model to predict  $D_0$  was obtained by first estimating  $D_0$  using individual-tree basal area increments for corresponding plots and measurement pairs used in the fit of the stand basal area model. The model was reparameterised so that the parameter to be

estimated is  $D_0^2$  rather than  $D_0$ . Model 11 then simply becomes

$$\begin{aligned} \partial G_{2k} &= c(D_{1k} - \sqrt{D_0^2}) ; D_{1k} > D_0 \\ &= 0 ; D_{1k} \leq D_0. \end{aligned}$$

This parameterisation ensures that  $\hat{D}_0 = \sqrt{(\hat{D}_0^2)}$  is positive. Also it has been found (P. West, pers. comm.) that  $\hat{D}_0^2$  has good statistical properties, with low bias and low values of the Lowry-Morton statistic (Ratkowsky 1983).

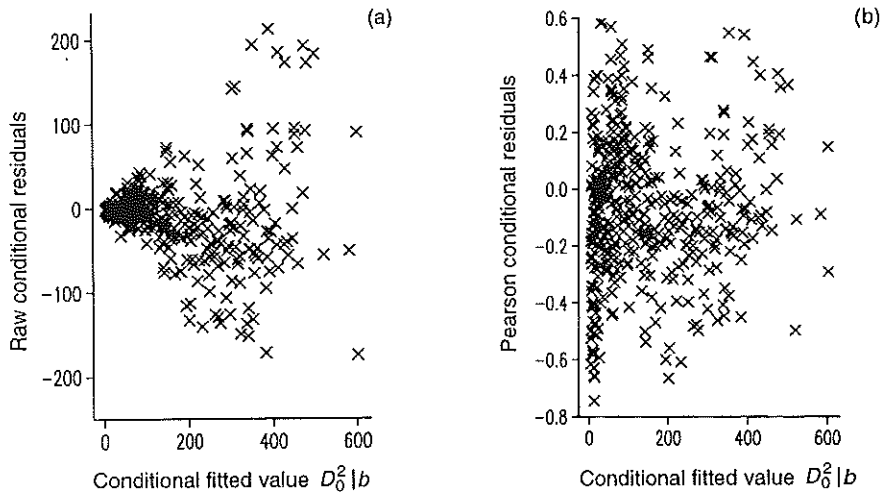


Figure 13. Conditional residuals for the individual-tree basal area increment model parameter,  $D_0^2$  (a) raw and (b) Pearson residuals.

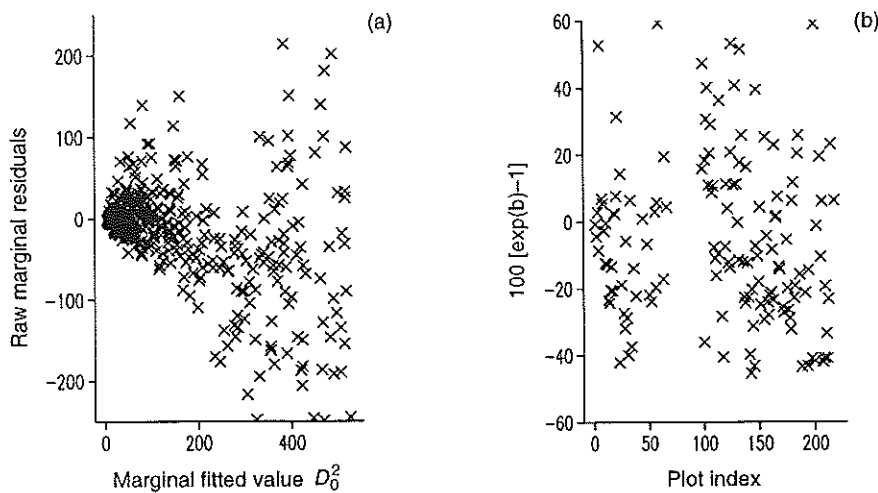


Figure 14. (a) Raw marginal residuals and (b) random plot effects estimates expressed as per cent deviations from the marginal mean for  $D_0^2$ .

The constraint (12) was imposed in the fitting procedure. The estimate of  $D_0^2$  indexed by plot  $i$  and measurement 2 in the pair was then modelled as a function of stand variables using the GLMM given by Model 14.

The marginal form of the model was fitted using the Genstat GLMM procedure. Table 8

gives the parameter estimates for (14), their standard errors and fit statistics. Figure 13a shows raw conditional residuals and Figure 13b shows Pearson conditional residuals versus conditional fitted values for  $\hat{D}_0^2$ . Figure 14a shows raw marginal residuals versus marginal fitted values while Figure 14b shows the random effects expressed as percentage

adjustments to the marginal fitted values versus plot index. It is clear from the above figures that although Model 14 is unbiased there is substantial between-plot (Figure 14b) and within-plot (Figure 13a) variability about predicted values of  $\hat{D}_0^2$  compared to the stand volume model (Figures 9 and 10).

### Tree-height regression parameter models

The final two models in the suite of models required to project yields and predict product assortments for *E. nitens* plantations are models of the parameters of the tree height to DBH regression. The simple log-reciprocal model of tree height as a function of DBH was fitted to each plot and measurement pair. The model for tree height,  $H_{Tk}$ , is given by

$$H_{Tk} = \exp(\beta_0 - \beta_1 D_k^{-1})$$

where  $H_{Tk}$  is the total height of the  $k$ th tree on the plot.

In a second stage, a mixed model was fitted to each of an exponential function of the estimated values of  $\beta_0$ , given by Model 15, and the estimated values of  $\beta_1$ , given by Model 16.

Models 15 and 16 were not fitted jointly so that any correlations between random effects  $b_{0i}$  and  $b_{1i}$  and between within-plot errors  $\varepsilon_0$  and  $\varepsilon_1$  are assumed to be zero. The fitting methodology could be improved by incorporating these correlations but this is not straightforward, requiring a multivariate mixed model approach. Models 15 and 16 were each fitted using Genstat's GLMM procedure with response variables  $\exp(\hat{\beta}_0)$

and  $\hat{\beta}_1$  with corresponding identity and log links respectively. Tables 9 and 10 give the parameter estimates for Models 15 and 16 respectively, along with their standard errors, and fit statistics. Figure 15a shows raw conditional residuals and Figure 15b shows Pearson conditional residuals versus conditional fitted values for  $\exp(\hat{\beta}_0)$ .

Figure 16a shows raw marginal residuals versus marginal fitted values while Figure 16b shows the random effects estimates versus plot index. Figure 17a shows raw conditional residuals and Figure 17b shows Pearson conditional residuals versus conditional fitted values for  $\hat{\beta}_1$ . Figure 18a shows raw marginal residuals versus marginal fitted values while Figure 18b shows the random effects expressed as percentage adjustments to the marginal fitted values versus plot index. From Figures 15 to 18, it

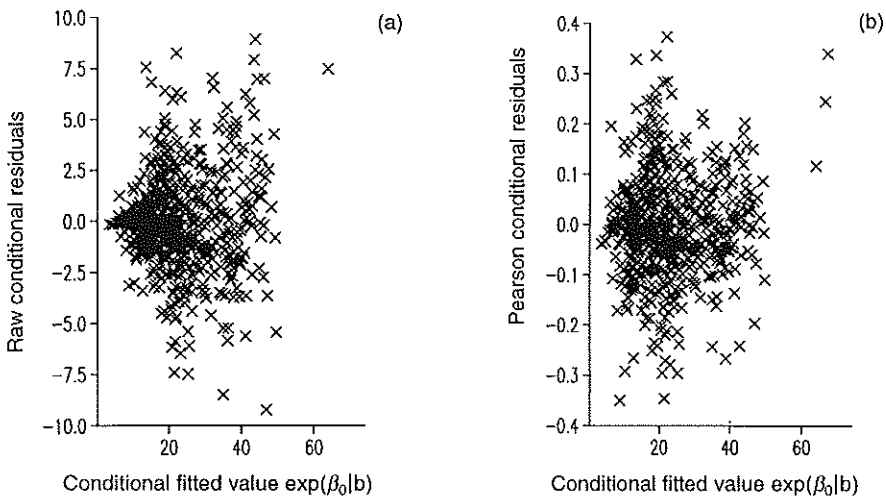


Figure 15. Conditional residuals for the tree height regression intercept parameter,  $\beta_0$  (a) raw, (b) Pearson residuals.

Table 9. Stand model for  $\exp(\beta_0)$ .

Parameter	$\beta_{00}$	$\beta_{01}$	$\beta_{02}$
Estimate	-3.8930	1.4030	-0.00211
Standard error	0.8854	0.0373	0.00059
Fit statistics	Value/estimate	Standard error	Effective df
Residual deviance	36.55	-	723.00
$\sigma_0^2$	21.3091	2.2707	213.59
$\phi_0$	0.0181	0.0011	509.41

Table 10. Stand model for  $\beta_1$ .

Parameter	$\beta_{10}$	$\beta_{11}$	$\beta_{12}$	$\beta_{13}$	$\beta_{14}$
Estimate	1.3650	0.0100	0.07787	-0.0612	-0.00029
Standard error	0.0845	0.0060	0.00966	0.0142	0.00006
Fit statistics	Value/estimate	Standard error	Effective df		
Residual deviance	157.5	-	716.00		
$\sigma_1^2$	0.1908	0.0212	213.54		
$\phi_1$	0.0690	0.0044	502.46		

**Model 15**

$$\exp(\hat{\beta}_0) = \beta_{00} + \beta_{01}H_{1i} + \beta_{02}N_{1i} + b_{0i} + \varepsilon_0 \quad (15)$$

**Model 16**

$$\hat{\beta}_1 = \exp(\beta_{10} + \beta_{11}Q_{1i} + \beta_{12}H_{1i} + \beta_{13}T_{1i} + \beta_{14}N_{1i} + b_{1i}) + \varepsilon_1 \quad (16)$$

where  $i$  represents the plot (the subscript for measurement is not shown),  $b_{0i}$  and  $b_{1i}$  are random plot effects with variances  $\sigma_0^2$  and  $\sigma_1^2$  respectively, and  $\varepsilon_0$  and  $\varepsilon_1$  are within-plot errors each assumed to be gamma distributed with dispersion parameters  $\phi_0$  and  $\phi_1$  respectively.

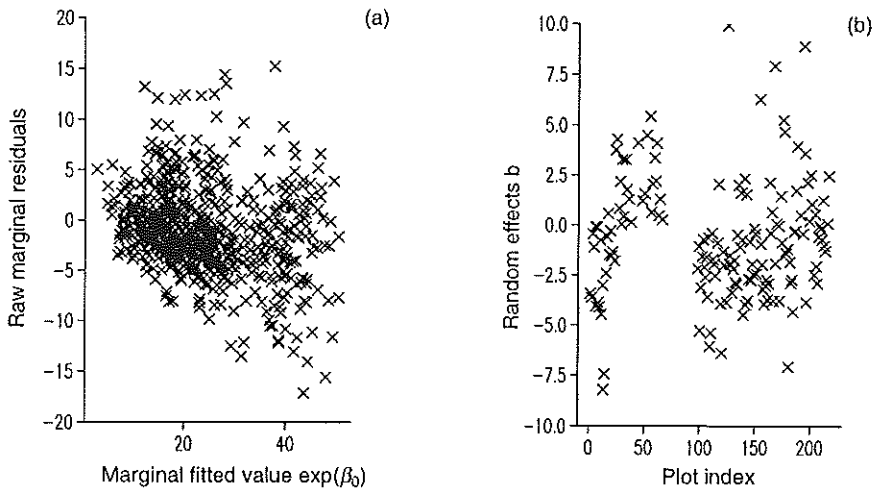


Figure 16. (a) Raw marginal residuals and (b) random plot effects estimates for height regression intercept parameter  $\beta_0$ .

can be seen that, as with the model of  $\hat{D}_0^2$ , there is a high degree of prediction error for both second-stage models, (15) and (16). This can be overcome to some degree by measuring a sample of tree heights as part of routine inventory, using temporary plots. Using the regression estimates of  $\exp(\beta_0)$  and  $\beta_1$  from this sample of tree heights and DBHs, an estimate of the random plot effect can be obtained for each of Models 15 and 16 by solving for  $b_0$  and  $b_1$ . For projections at ages after inventory, these random plot effects can be used to adjust marginal model predictions using (15) and (16).

## Discussion

The most important limitation of the models developed above is the lack of data at older ages. For sawlog regimes with rotation ages up to around 45 years (Candy and Gerrard 1997), the restricted range of ages shown in Figure 1 means that predicted trajectories over age 20 are extrapolations of the data and should be used with caution. As well as this limitation, to provide a dataset which was sufficient for growth modelling, plot data from a wide geographic range of sites in Tasmania and New Zealand were combined. Differences

in growth trajectories between geographic regions have not been modelled explicitly here. However, when the models are applied in their projection form, some of this regional variation will be incorporated via the initial conditions obtained from inventory. Given these conditions, models of the type described here assume predicted growth trajectories are unbiased irrespective of establishment techniques, site attributes, or genetic stock. These assumptions can be tested using regional data, while a revision of the models should be carried out when the permanent plots used in this study have had further measurements over the next, say, 10 to 15 years. Also, a project to test the New Zealand taper model used here, and adjust it if necessary, for different regions and regimes is a high priority.

Projecting stand basal area accurately is the most important single determinant of the overall accuracy of the output of primary interest, stand volume, given data such as that used here. Figure 7 demonstrates a key property of the stand basal area projection model; that is, the sensitivity of projections to initial basal area for the projection period,  $B_1$ . For example, where the initial basal area is high relative to stands of the same age at the start of the period, then projected growth will be high while the actual growth rate may decline. Conversely, stands with relatively



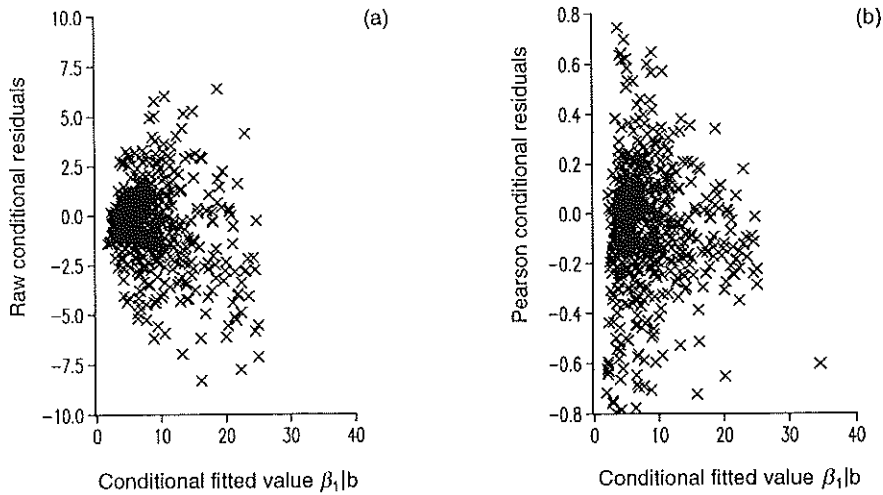


Figure 17. Conditional residuals for the tree height regression slope parameter,  $\beta_1$  (a) raw and (b) Pearson residuals.

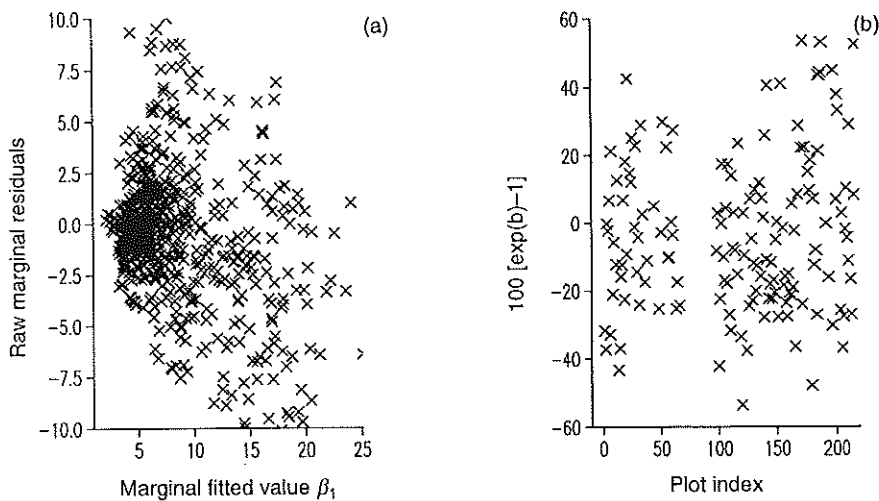


Figure 18. (a) Raw marginal residuals and (b) random plot effects estimates expressed as per cent deviations from the marginal mean for  $\beta_1$ .

low initial basal area will produce low projected growth. Considering unthinned stands for simplicity, initial basal area at a given age is used implicitly in the model as a measure of site quality, given initial stocking is adequate to produce full site occupancy at a reasonably young age (e.g. by age five to eight). This is in addition to the effect of site

index in the model and is the dominant effect on stand basal area projections. Considering again Figure 7, if the initial basal area was set to a later age than the first measurement of the plot after age three, then projections will more accurately reflect the actual basal area trajectory from initial age. The general principle in the state-space approach (Garcia

1994) is that the state variables solely determine future states; however, if stand basal area does not reflect the site's productivity, taking thinning into account, then predicted and realised stand basal area trajectories may diverge substantially over long projection periods.

There are many reasons why stand basal area may not adequately reflect the site's productivity given adequate stocking. These include underestimation of site productivity due to poor establishment, episodes of insect attack, and atypically poor growing conditions for the site. Conversely, overestimation can occur because of atypically good early growing conditions such as short-term improvement of soil nutrients by fertilisation or because a site factor (e.g. shallow soil depth) does not limit growth until later in the rotation.

One way to improve the situation is to delay inventory as long as possible without limiting its utility for yield scheduling. If an inventory is not carried out at any scheduled thinning, inventory should be delayed until at least three to five years after thinning to allow stand basal area at this time to have incorporated any thinning response. Projections for individual inventory plots will always be subject to large errors; for example, an error of approximately 40% of projected basal area for the age 10 to 30 projection period was given earlier. However, if the model projections are unbiased given inputs, averaging projections for a sample of inventory plots can produce estimates at the total resource or regional level which are relatively accurate given a sufficiently large sample of inventory plots.

Simulations of hypothetical stands for silvicultural regime evaluation can be carried out using the models if an estimate of site index is available. The difficulty in this case is that site index can only be estimated reliably for existing stands using inventory plots. This problem can be alleviated by development of a 'hybrid empirical/mechanistic' model

which can predict site index from a site productivity measure based on GIS-captured data (where possible) independent of current land-use at a given site. To allow evaluation of financial returns from future plantations of *E. nitens*, development of such a model is a high priority.

Mixed model approaches to model fitting and testing have been used extensively in this study. For all the models where random plot effects were incorporated, these effects were a highly significant source of variation in addition to the between measurement (within-plot) source of random error. Taking into account the variation due to random plot effects has allowed more rigorous hypothesis tests for model selection, more accurate estimation of prediction error variances, and appropriate adjustment for back-transformation bias in the case of the stand basal area projection model. Further work is required to determine if the assumed independent conditional error structure is adequate. For example, a continuous autoregressive error structure conditional on random plot effects could be employed (Gregoire *et al.* 1995). This has not been done to the author's knowledge for a projection model.

### Acknowledgements

The co-operation of the organisations that contributed data to this project is greatly appreciated. Thanks are due in particular to Heather McKenzie and Wai Mason (Forest Research Institute, Rotorua, New Zealand), Bernard Walker, Brett Miller, and Jeremy Wilson (North Forests Burnie), Dr Chris Beadle and Charles Turnbull (retired) (CSIRO Division of Forestry), and Adam Gerrand (Forestry Tasmania). Dr Humphrey Elliott and Dr Timothy Gregoire kindly reviewed the manuscript and their comments are appreciated. A special vote of thanks to Wengui Su for his help in preparing the data for modelling. This project was jointly funded by the Intensification of Forest Management Project and Forestry Tasmania.

## References

- Bailey, R.L. and Ware, K.D. (1983). Compatible basal area growth and yield model for thinned and unthinned stands. *Canadian Journal of Forest Research* 13: 563–571.
- Beadle, C.L., McLeod, D.E., Turnbull, C.R.A., Ratkowsky, D.A. and McLeod, R. (1989). Juvenile/total foliage ratios in *Eucalyptus nitens* and the growth of stands and individual trees. *Trees* 3: 117–124.
- Beadle, C.L. and Turnbull, C.R.A. (1986). Leaf and branch development in two contrasting species of *Eucalyptus* in relation to early growth and biomass production. In: *Crown and Canopy Structure in Relation to Productivity* (eds T. Fujimori and D. Whitehead), pp. 263–283. Forestry and Forest Products Research Institute, Ibaraki, Japan.
- Breslow, N.E. and Clayton, D.G. (1993). Approximate inference in generalized linear mixed models. *Journal of the American Statistical Association* 88: 9–25.
- Campbell, R.G., Ferguson, I.S. and Opie, J.E. (1979). Simulating growth and yield of mountain ash stands: a deterministic model. *Australian Forest Research* 9: 189–202.
- Candy, S.G. (1989). Growth and yield models for *Pinus radiata* in Tasmania. *New Zealand Journal of Forestry Science* 19: 112–133.
- Candy, S.G. (1997). Estimation in forest yield models using composite link functions with random effects. *Biometrics* 53: 146–160.
- Candy, S.G. and Gerrand, A. (1997). Comparison of financial returns from sawlog regimes for *Eucalyptus nitens* plantations in Tasmania. *Tasforests* 9: 35–50.
- Clutter, J.L., Fortson, J.C., Pienaar, L.V., Brister, G.H. and Bailey, R.L. (1983). *Timber Management, a Quantitative Approach*. John Wiley and Sons, New York.
- Davidian, M. and Gallant, A.R. (1993). The nonlinear mixed effects model with a smooth random effects density. *Biometrika* 80: 475–488.
- Engel, B. and Keen, A. (1994). A simple approach for the analysis of generalized linear mixed models. *Statistica Neerlandica* 48: 1–22.
- Flewelling, J.W. and Pienaar, L.V. (1981). Multiplicative regression with lognormal errors. *Forest Science* 27: 281–289.
- Garcia, O. (1984). New class of growth models for even-aged stands: *Pinus radiata* in Golden Downs forest. *New Zealand Journal of Forest Research* 13: 267–270.
- Garcia, O. (1994). The state-space approach in growth modelling. *Canadian Journal of Forest Research* 24: 1894–1903.
- Genstat 5 Committee (1993). *Genstat 5 Reference Manual*. Clarendon Press, Oxford.
- Gerrand A.M., Medhurst, J.L. and Neilsen, W.A. (1997). Thinning and pruning eucalypt plantations for sawlog production in Tasmania. *Tasforests* 9: 15–34.
- Goulding, C.J. (1986). Measurement of tree crops. In: *Forestry Handbook* (ed. H. Levack), pp. 80–81. New Zealand Institute of Foresters, Wellington North, New Zealand.
- Gregoire, T.G., Schabenberger, O. and Barrett, J.P. (1995). Modelling irregularly spaced, unbalanced, longitudinal data from permanent plot measurements. *Canadian Journal of Forest Research* 25: 137–156.
- Hallam, P.M., Reid, J.B. and Beadle, C.L. (1989). Frost hardness of six potential plantation *Eucalyptus* species. *Canadian Journal of Forest Research* 19: 1235–1239.
- Hyink, D.M. and Moser, J.W. Jr (1983). A generalized framework for projecting forest yield and stand structure using diameter distributions. *Forest Science* 29: 85–95.
- Knoebel, B.R., Burkhart, H.E. and Beck, D.E. (1986). A growth and yield model for thinned stands of yellow-poplar. *Forest Science Monograph* 27.
- Lindstrom, M.J. and Bates, D.M. (1990). Nonlinear mixed effects models for repeated measures data. *Biometrics* 46: 673–687.
- Macalister, P. (1995). 'Gums gain'. *New Zealand Forestry Industries Journal* 12: 12–13.
- McCullagh, P. and Nelder, J.A. (1989). *Generalized Linear Models* (2nd ed.). Chapman and Hall, London.
- McGilchrist, C.A. (1994). Estimation in generalized mixed models. *Journal of the Royal Statistical Society B* 56: 61–69.
- McMullan, M.J. (1979). Overall measurement systems for exotic plantations NSW Forestry Commission. In: *Mensuration for Management Planning of Exotic Forest Plantations* (compiler D.A. Elliott), pp. 77–87. Proceedings of Symposium No. 20, New Zealand Forest Research Institute.
- Payne, R.W., Arnold, G.M. and Morgan, G.W. (eds) (1993). *Genstat 5 Procedure Library Manual*. Release 3[1]. Lawes Agricultural Trust (Rothamsted Experimental Station).
- Pienaar, L.V. and Shiver, B.D. (1986). Basal area prediction and projection equations for pine plantations. *Forest Science* 32: 626–633.

- Ratkowsky, D.A. (1983). *Nonlinear Regression Analysis*. Dekker, New York.
- Robinson, G.K. (1991). That BLUP is a good thing: the estimation of random effects. *Statistical Science* 6: 15–51.
- Schabenberger, O. and Gregoire T.G. (1996). Population-averaged and subject-specific approaches for clustered categorical data. *Journal Statistical Computation Simulation* 54: 231–253.
- Schall, R. (1991). Estimation in generalized linear models with random effects. *Biometrika* 78: 719–727.
- Searle, S.R. (1965). *Matrix Algebra for the Biological Sciences*. John Wiley and Sons, London.
- Turnbull, C.R.A., Beadle, C.L., Bird, T. and McLeod, D.E. (1988). Volume production in intensively-managed eucalypt plantations. *Appita* 41: 447–450.
- Turnbull, C.R.A., McLeod, D.E., Beadle, C.L., Ratkowsky, D.A., Mummery, D.C. and Bird, T. (1993). Comparative growth of *Eucalyptus* species of the subgenera *Symphylomyrtus* and *Monocalyptus*. *Australian Forestry* 56: 276–286.
- Vonesh, E.F. and Carter, R.L. (1992). Mixed-effects nonlinear regression for unbalanced repeated measures. *Biometrics* 48: 1–17.
- Wedderburn, R.W.M. (1974). Quasilikelihood functions, generalized linear models and the Gauss-Newton method. *Biometrika* 61: 439–447.
- West, P.W., Ratkowsky, D.A. and Davis, A.W. (1984). Problems of hypothesis testing with multiple measurements from individual sampling units. *Forest Ecology and Management* 7: 207–224.
- Whyte, I.N. (1992). The current eucalypt plantation resource in temperate Australia and future development. Paper delivered to the CRC seminar *The Role and Potential of Eucalypt Plantations in Australia's Wood Supply*.
- Wolfinger, R. and O'Connell, M. (1993). Generalized linear mixed models: a pseudo-likelihood approach. *Journal of Statistical Computing and Simulation* 48: 233–243.
- Wolfinger, R. (1993). Laplace's approximation for nonlinear mixed models. *Biometrika* 80: 791–795.
- Woolons, R.C. and Hayward, W.J. (1985). Revision of a growth and yield model for radiata pine in New Zealand. *Forest Ecology and Management* 11: 191–202.
- Zeger, S.L., Liang, K.Y. and Albert, P.S. (1988). Models for longitudinal data: a generalized estimating equation approach. *Biometrics* 44: 1049–1060.

## Appendix 1. Fitting the algorithm for the nonlinear mixed model of stand basal area

To fit Model 4 as a NLMM, the following procedure was used. The procedure involves linearisation of (4) using a Taylor series expansion and then iteration between a generalised least squares (GLS) fit of fixed effect parameters combined with Best Linear Unbiased Prediction (BLUP) (Robinson 1991) of the random effects and REML estimation of the variance components (see Breslow and Clayton (1993) for the corresponding GLMM procedure and Candy (1997) for the composite link GLMM case). The subject-specific method is derived first from which the marginal method (Breslow and Clayton 1993) is developed. The steps in the fitting procedure are:

**Step 1.** Taylor series expansion of the nonlinear model and calculation of working response and predictor variables.

For the subject-specific model with response  $\ln(B_{2i})$ , the conditional mean,  $\mu_b$  (dropping the  $i$  subscript for simplicity of notation), is given by

$$\mu_b = E\{\ln(B_2) \mid \mathbf{v}, \alpha_0, \dots, \alpha_5, b_1, b_2\}$$

where  $\mathbf{v}$  represents the vector of predictor variables  $(B_1, T_1, T_2, S, T_t, P_t)$ ,

and its estimate at the  $r$ th iteration of the fitting algorithm is

$$\mu_b^{(r)} = E\{\ln(B_2) \mid \mathbf{v}, \alpha_0^{(r)}, \dots, \alpha_5^{(r)}, b_1^{(r)}, b_2^{(r)}\}$$

or in terms of the model

$$\mu_b^{(r)} = \left( \frac{\eta_1^{(r)}}{\eta_2^{(r)}} \right)^{\alpha_2} \ln(B_1) + \left( \alpha_0^{(r)} + \alpha_1^{(r)} S_t + b_1^{(r)} \right) \left\{ 1 - \left( \frac{\eta_1^{(r)}}{\eta_2^{(r)}} \right)^{\alpha_2} \right\}$$

where

$$\begin{aligned} \eta_1^{(r)} &= T_1 + \alpha_3^{(r)} P_t + \alpha_4^{(r)} P_t T_t + \alpha_5^{(r)} P_t T_t S + b_2^{(r)} \\ \eta_2^{(r)} &= T_2 + \alpha_3^{(r)} P_t + \alpha_4^{(r)} P_t T_t + \alpha_5^{(r)} P_t T_t S + b_2^{(r)}. \end{aligned}$$

Since there are  $n$  parameters to be estimated for each of the random effects  $b_1$  and  $b_2$ , let the vector  $\mathbf{b}$  be the length  $2n$  stacked vector of plot random effects so that  $\mathbf{b} = (b_{1,1}, b_{2,1} \mid \dots \mid b_{1,n}, b_{2,n})'$ .

Expanding  $\mu_b^{(r)}$  about  $\mu_b^{(r-1)}$  using a first-order Taylor series expansion gives

$$\mu_b^{(r)} = \mu_b^{(r-1)} + \sum_{s=0}^5 \left[ \frac{\partial \mu_b}{\partial \alpha_s} \right]_{\alpha_s = \alpha_s^{(r-1)}} (\alpha_s^{(r)} - \alpha_s^{(r-1)}) + \sum_{t=1}^{2n} \left[ \frac{\partial \mu_b}{\partial b_t} \right]_{b_t = b_t^{(r-1)}} (b_t^{(r)} - b_t^{(r-1)}) \quad (\text{A1})$$

and specifying the model as

$$\ln(B_2) = \mu_b^{(r)} + \varepsilon \quad (\text{A2})$$

this model can be fitted by regressing working response variable,  $y$ , on working fixed design matrix  $\mathbf{X}$  and

working random design matrix  $Z$ , where

$$y = \left\{ \ln(B_2) - \mu_b^{(r-1)} \right\} + \sum_{s=0}^5 \left[ \frac{\partial \mu_b}{\partial \alpha_s} \right]_{\alpha_s = \alpha_s^{(r-1)}} \alpha_s^{(r-1)} + \sum_{t=1}^{2n} \left[ \frac{\partial \mu_b}{\partial b_t} \right]_{b_t = b_t^{(r-1)}} b_t^{(r-1)},$$

the columns of the design matrix for the  $i$ th plot,  $X_i$ , are given by

$$\left[ \frac{\partial \mu_b}{\partial \alpha_s} \right]_{\alpha_s = \alpha_s^{(r-1)}} ; s = 0, 1 \dots 5$$

and similarly for  $Z_i$  by

$$\left[ \frac{\partial \mu_b}{\partial b_t} \right]_{b_t = b_t^{(r-1)}} ; t = 1, \dots, 2n.$$

The size of  $X$  is  $N \times 6$  where  $N$  is the total number of plot measurements,  $N = \sum_{i=1}^n m_i$  and  $m_i$  is the number of measurements on the  $i$ th plot, and there are a total of  $n$  plots so that  $X$  is formed by 'stacking' the individual plot design matrices  $X_i$ ;  $i = 1, \dots, n$ .  $Z$  is the  $N \times 2n$  random-effects design matrix with  $Z = (Z_1 \oplus Z_2 \oplus \dots \oplus Z_n)$  the direct sum (Searle 1965) of the  $Z_i, i = 1, \dots, n$  where  $Z_i$  is an  $m_i \times 2$  matrix. The working response vector,  $y$ , is size  $N \times 1$  and is formed by stacking the  $n$  individual plot vectors.

**Step 2.** Updating estimates of the fixed-effect and random-effect parameters. The conditional variance of  $y$  is assumed to be

$$\text{Var}(y | \mathbf{v}, \alpha_0^{(r-1)}, \dots, \alpha_5^{(r-1)}, b_1^{(r-1)}, b_2^{(r-1)}) = \left\{ 1 - \left( \frac{\eta_1^{(r-1)}}{\eta_2^{(r-1)}} \right)^{\alpha_2} \right\}^2$$

so let the  $(N \times N)$  diagonal weight matrix  $W$  have diagonal element

$$W(ij, ij) = \phi^{-1} w^2 = \phi^{-1} \left\{ 1 - \left( \frac{\eta_1^{(r-1)}}{\eta_2^{(r-1)}} \right)^{\alpha_2} \right\}^{-2}$$

The six fixed-effect and  $2n$  random-effect parameters are estimated from the following mixed model equations

$$X' W X \alpha^{(r)} + X' W Z b^{(r)} = X' W y$$

$$Z' W X \alpha^{(r)} + (Z' W Z + D_K^{-1}) b^{(r)} = Z' W y$$

where  $D_K$  is block-diagonal with elements,  $\phi D_\lambda$  where  $D_\lambda = \text{diag}(\lambda_1, \lambda_2)$ , involving the scaled variance

components given by  $\lambda_1 = \frac{\sigma_1^2}{\phi}$ ,  $\lambda_2 = \frac{\sigma_2^2}{\phi}$  where  $\phi = \sigma^2$ . The dispersion parameter,  $\phi$ , can be factored out of the mixed model equations and estimated at convergence. The estimates of  $\lambda_1$  and  $\lambda_2$  were obtained from the previous iteration's calculation of step (3) below.

The solution of the mixed model equations gives a GLS estimator to update the fixed-effect parameters as

$$\tilde{\alpha}^{(r)} = (\mathbf{X}' \mathbf{Q}^{-1} \mathbf{X})^{-1} \mathbf{X}' \mathbf{Q}^{-1} \mathbf{y}$$

where

$$\mathbf{Q} = \mathbf{Z} \mathbf{D}_K \mathbf{Z}' + \mathbf{W}^{-1}$$

and BLUP of the random effects is given by

$$\hat{\mathbf{b}} = \mathbf{D}_K \mathbf{Z}' \mathbf{Q}^{-1} (\mathbf{y} - \mathbf{X} \tilde{\alpha}^{(r)}).$$

Note that we could scale  $\mathbf{y}$ ,  $\mathbf{X}$  and  $\mathbf{Z}$  in the mixed model equations by multiplying each by the weight  $w^{\frac{1}{2}}$  so that  $\mathbf{W}$  then becomes the identity matrix. This scaling was carried out for the fit described in the text.

Convergence is tested by the change in the residual sum of squares, *RSS*,

$$RSS = \sum_{i=1}^n \sum_{j=2}^m (B_{ji} - \hat{B}_{ji})^2.$$

The estimate of  $\alpha$  is damped before it is used to update values of  $\mathbf{y}$ ,  $\mathbf{X}$ ,  $\mathbf{Z}$  and  $w$  in the next iteration. The damped estimate is given by

$$\hat{\alpha}^{(r)} = 0.5 \tilde{\alpha}^{(r)} + 0.5 \hat{\alpha}^{(r-1)}$$

if the *RSS* decreases from iteration  $r-1$  to  $r$ , and

$$\hat{\alpha}^{(r)} = 0.1 \tilde{\alpha}^{(r)} + 0.9 \hat{\alpha}^{(r-1)}$$

if the *RSS* increases.

**Step 3.** The REML estimation procedure was used to estimate  $\lambda_1$  and  $\lambda_2$  (see Candy 1997). The dispersion parameter is calculated at convergence as follows

$$\hat{\phi} = (\mathbf{y} - \mathbf{X} \hat{\alpha}^{(r)} - \mathbf{Z} \hat{\mathbf{b}}^{(r)})' \mathbf{W} (\mathbf{y} - \mathbf{X} \hat{\alpha}^{(r)} - \mathbf{Z} \hat{\mathbf{b}}^{(r)}) (N - 6 - 2n + v)^{-1}$$

where  $v$  corresponds to Schall's (1991)  $v_1$ .

#### *The marginal model*

Fitting the marginal model requires the simple adjustment whereby the random effects estimates are excluded from, or equivalently set to zero in, the calculation of  $\mathbf{y}$ ,  $\mathbf{X}$  and  $\mathbf{Z}$  in Step 1 and  $w$  in Step 2. However, the BLUPs of the random effects  $\hat{\mathbf{b}}^{(r)}$  are still required to estimate  $\lambda_1, \lambda_2, \phi$  in Step 3 and therefore  $\hat{\alpha}^{(r)}$  in Step 2. The assumption is made (Breslow and Clayton 1993) in doing this that the

conditional or subject-specific value of the response  $\mu_b$  is well approximated by the marginal value  $\mu = E\{\ln(B_2) | \mathbf{v}, \alpha_0, \dots, \alpha_5\}$ . Substituting  $\mu$  for  $\mu_b$  in (A1) and excluding random effects from the calculation of  $\mathbf{y}$ ,  $\mathbf{X}$  and  $\mathbf{Z}$  is equivalent to setting  $b_t^{(r-1)} = 0$ ;  $t = 1, \dots, 2n$ . At convergence, the variance of the response based on (A1) and (A2) is approximately

$$\text{Var}\{\ln(B_2)\} \equiv \text{Var}(\mathbf{y}) = \mathbf{ZD}_K\mathbf{Z}' + \phi\mathbf{W}^{-1}.$$

So in the marginal fitting algorithm, the previous iteration's value of  $\mathbf{b}$  is not needed to update  $\mu^{(r)}$ ; only the previous iteration's estimates of  $\lambda_1$  and  $\lambda_2$  are required to calculate  $\hat{\alpha}^{(r)}$  and thus  $\mu^{(r)}$ .

The alternative is to fit the SS model and adjust the SS fixed-effect parameter estimates to give population-average values (Zeger *et al.* 1988) but this is not easy to do in the case of a NLMM. The procedure used here was implemented in Genstat with Steps 2 and 3 using the REML directive.

## Appendix 2. Adjustment for back-transformation bias in the stand basal area projection model.

The predicted value of stand basal area obtained from Model 4 is given on the logarithmic scale. To obtain the prediction of stand basal area, the result from (4) must be back-transformed using the exponential function. To correct for back-transformation bias, the following correction to  $\hat{B}_2 = \exp\{\hat{\mu}\}$  was given earlier as Equation 6:

$$\bar{B}_2 = \exp\left\{0.5(\sigma_1^2 z_1^2 + \sigma_2^2 z_2^2 + w^{-1}\sigma^2)\right\} \hat{B}_2.$$

This result is now derived.

For repeated sampling of the theoretical population of plots with site index  $S$  and fixing the projection period and thinning variables, if the random variable  $\ln(Y^*) = \ln(B_2)$  has a normal distribution with conditional mean for  $Y^*$

$E(Y^* | \mathbf{v}, \alpha_0, \dots, \alpha_5, b_1, b_2) = \exp\left(\mu_b + \frac{w^{-1}\sigma^2}{2}\right)$ , then approximating  $\mu_b$  by  $\mu_b^{(r)}$  at convergence of the fitting algorithm in Appendix 1, the marginal mean of  $B_2$  can be approximated as follows:

$$\begin{aligned} E(B_2) &\equiv \int_{-\infty}^{\infty} C \exp\left(\mu^{(r)} + \left\{ \mathbf{z}\mathbf{b} + \frac{w^{-1}\sigma^2}{2} \right\}\right) \exp\left(-\left\{2\sigma^2\right\}^{-1} \mathbf{b}' \mathbf{D}_\lambda^{-1} \mathbf{b}\right) d\mathbf{b} \\ &= \exp\left\{0.5(\sigma_1^2 z_1^2 + \sigma_2^2 z_2^2 + w^{-1}\sigma^2)\right\} \exp\left(\mu^{(r)}\right) \end{aligned}$$

where

$$\mathbf{z} \text{ is a row of } \mathbf{Z} \text{ and } C = (2\pi)^{-1} |\mathbf{D}_\lambda|^{-\frac{1}{2}}.$$

If we substitute estimated values in the above expression we get Equation 6.